Quantum tunneling in nuclear fusion

A. B. Balantekin

Department of Physics, University of Wisconsin-Madison, Madison, Wisconsin 53706

N. Takigawa

Department of Physics, Tohoku University, 980-77 Sendai, Japan

Recent theoretical advances in the study of heavy-ion fusion reactions below the Coulomb barrier are reviewed. Particular emphasis is given to new ways of analyzing data (such as studying barrier distributions), new approaches to channel coupling (such as the path-integral and Green's function formalisms), and alternative methods to describe nuclear structure effects (such as those using the interacting boson model). The roles of nucleon transfer, asymmetry effects, higher-order couplings, and shape phase transitions are elucidated. The current status of the fusion of unstable nuclei and very massive systems are briefly discussed.
[S0034-6861(98)00301-8]

CONTENTS

I. INTRODUCTION

Quantum tunneling in systems with many degrees of freedom is one of the fundamental problems in physics and chemistry (Hänggi *et al.*, 1990; Tsukada *et al.*, 1993). One example of a tunneling phenomenon in nuclear physics is the fusion of two nuclei at very low energies. These reactions are not only of central importance for stellar energy production and nucleosynthesis, but they also provide new insights into reaction dynamics and nuclear structure. Until about fifteen years ago, low-energy fusion reactions were analyzed in terms of a simple model, in which one starts with a local, one-dimensional real potential barrier formed by attractive nuclear and repulsive Coulomb interactions and assumes that absorption into the fusion channel takes place in the region inside the barrier after the quantum tunneling. The shape, location, and height of this potential were described in terms of a few parameters which were varied to fit the measured cross sections. The systematics of potentials obtained in this way were discussed by Vaz *et al.* (1981). A number of experiments performed in the early eighties showed that the subbarrier fusion cross sections for intermediate-mass systems are much larger than those expected from such a simple picture (Beckerman, 1988; Vandenbosch, 1992). The inadequacy of the one-dimensional model for subbarrier fusion was explicitly demonstrated by inverting the experimental data to directly obtain the effective one-dimensional fusion barrier under the constraint that it be energy independent (Balantekin *et al.*, 1983).

In recent years much experimental effort has been devoted to measuring fusion cross sections and moments of compound-nucleus angular momentum distributions. A complete compilation of the recent data is beyond the scope of this review. Several recent reviews (Reisdorf, 1994; Stefanini, 1994) present an excellent overview of the current experimental situation. This article reviews theoretical developments of the last decade which have enhanced our understanding of the multidimensional quantum tunneling nature of subbarrier fusion. We should emphasize that the large volume of new data and extensive theoretical work does not allow us to provide an exhaustive set of references. The selection we made does not imply that omitted references are any less important than the ones we chose to highlight in discussing different aspects of fusion phenomena.

The natural language for studying fusion reactions below the Coulomb barrier is the coupled-channels formalism. In the last decade coupled-channels analysis of the data and the realization of the connection between energy derivatives of the cross section and the barrier dis-

tributions (Rowley *et al.*, 1991) have motivated accumulation of very-high-precision data.

When the enhancement of the cross section below the barrier was first observed, many authors pointed out that it is not easy to identify the underlying physical mechanism (Brink, *et al.*, 1983; Krappe *et al.*, 1983). Any coupling introduced between translational motion and internal degrees of freedom enhances the cross section. The recent high-precision data helped resolve some of these ambiguities by studying barrier distributions and mean angular momenta as well. The quality of the existing data now makes it possible to explore quantitatively a number of theoretical issues in the quantum tunneling aspects of subbarrier fusion, such as effects of anharmonic and nonlinear interaction terms.

In the next section, after briefly reviewing observables accessible in heavy-ion fusion reactions, and the reasons why a one-dimensional description fails, we present the motivation for studying barrier distributions. In Sec. III we discuss the standard coupled-channels formalism and alternative approaches such as the path-integral formalism and Green's-function approaches along with their various limiting cases. Section IV has a dual purpose: it covers recent attempts to describe nuclear structure effects using the interacting boson model while illustrating the technical details of the alternative approaches discussed in Sec. III. In Sec. V, we survey a representative sample of recent high-quality data with a focus on new physics insights. We conclude in Sec. VI with a brief discussion of the open problems and outlook for the near future.

II. ONE-DIMENSIONAL MODEL FOR FUSION

A. Experimental observables

In the study of fusion reactions below the Coulomb barrier the experimental observables are the cross section

$$\sigma(E)=\sum_{\ell=0}^{\infty}\sigma_\ell(E) \tag{1}$$

and the average angular momenta

$$\langle \ell(E)\rangle=\frac{\Sigma_{\ell=0}^{\infty}\ell\,\sigma_\ell(E)}{\Sigma_{\ell=0}^{\infty}\sigma_\ell(E)}. \tag{2}$$

The partial-wave cross sections are given by

$$\sigma_\ell(E)=\frac{\pi\hbar^2}{2\mu E}(2\ell+1)T_\ell(E), \tag{3}$$

where $T_\ell(E)$ is the quantum-mechanical transmission probability through the potential barrier and μ is the reduced mass of the projectile and target system.

Fusion cross sections at low energies are measured by detecting evaporation residues or fission products from compound nucleus formation. Evaporation residues can be detected directly by measuring the difference in velocities between them and the beamlike ions. Velocity selection can be achieved either by electrostatic deflectors or by velocity filters. Alternative techniques include detecting either direct or delayed x rays and gamma rays. A review of different experimental techniques for measuring the fusion cross sections is given by Beckerman (1988).

Several techniques were developed for measuring moments of the angular momentum distributions. The advent of detector arrays made possible the measurement of full gamma-ray multiplicities (Fischer *et al.*, 1986; Halbert *et al.*, 1989), which, under some assumptions, can be converted to σ_ℓ distributions. It is also possible to measure relative populations of the ground and isomeric states in the evaporation residues to deduce the spin distribution in the compound nucleus (Stokstad *et al.*, 1989; DiGregorio *et al.*, 1990). Finally, the anisotropy of the fission-fragment angular distribution can be related to the second moment of the spin distribution (Back *et al.*, 1985; Vandenbosch *et al.*, 1986a, 1986b).

It is worthwhile to emphasize that moments of angular momenta, unlike the fusion cross section itself, are not directly measurable quantities. One needs to make a number of assumptions to convert gamma-ray multiplicities or isomeric state populations to average angular momenta. An elaboration of these assumptions along with a thorough discussion of the experimental techniques is given by Vandenbosch (1992).

B. One-dimensional barrier penetration

The total potential between the target and projectile nuclei for the ℓth partial wave is given by

$$V_\ell(r)=V_N(r)+V_C(r)+\frac{\hbar^2\ell(\ell+1)}{2\mu r^2}$$
$$=V_0(r)+\frac{\hbar^2\ell(\ell+1)}{2\mu r^2}, \tag{4}$$

where V_N and V_C are the nuclear and Coulomb potentials, respectively. The $\ell=0$ barrier is referred to as the Coulomb barrier. The barriers obtained in Eq. (4) are illustrated in Fig. 1 for several ℓ values.

For a one-dimensional barrier, transmission probabilities can be evaluated numerically—either exactly or using a uniform WKB approximation, valid for energies both above and below the barrier (Brink and Smilansky, 1983a; Brink, 1985a):

$$T_\ell(E)=\{1+\exp[2S_\ell(E)]\}^{-1}, \tag{5}$$

where the WKB penetration integral is

$$S_\ell(E)=\sqrt{\frac{2\mu}{\hbar^2}}\int_{r_{1\ell}}^{r_{2\ell}}dr\left[V_0(r)+\frac{\hbar^2\ell(\ell+1)}{2\mu r^2}-E\right]^{1/2}. \tag{6}$$

In this equation $r_{1\ell}$ and $r_{2\ell}$ are the classical turning points for the ℓth partial-wave potential barrier.

If we assume that the potential barrier can be replaced by a parabola

$$V_0(r)=V_{B0}-\tfrac{1}{2}\mu^2\Omega^2(r-r_o)^2, \tag{7}$$

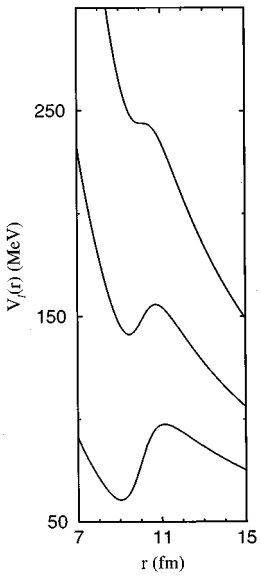

FIG. 1. One-dimensional potential of Eq. (4) for the ^{64}Ni+^{64}Ni system for several ℓ values. The lowest barrier is for $\ell=0$ (the bare barrier). The middle and top barriers are for $\ell=100$ and $\ell=150$, respectively.

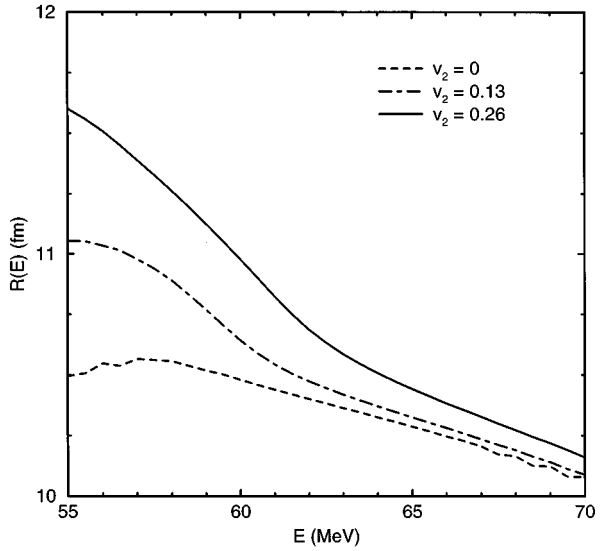

FIG. 2. The effective radius extracted from fusion calculations for the ^{16}O+^{154}Sm system using Eq. (6). The curves correspond to spherical, vibrational, and deformed nuclei with quadrupole coupling strengths $v_2=0$, 0.13, and 0.26, respectively. From Balantekin *et al.* (1996).

where V_{B0} is the height and Ω is a measure of the curvature of the s-wave potential barrier, the transmission probability can be calculated to be (Hill and Wheeler, 1953)

$$T_0(E)=\left\{1+\exp\left[-\frac{2\pi}{\hbar\Omega}(E-V_{B0})\right]\right\}^{-1}. \tag{8}$$

In the nuclear physics literature Eq. (8) is known as the Hill-Wheeler formula. Especially at energies well below the barrier there are significant deviations from this formula as the parabolic approximation no longer holds.

C. Barrier distributions

An alternative way of plotting the total cross-section data is to look at the second energy derivative of the quantity $E\sigma$, sometimes called the distribution of the barriers. To elaborate on the physical significance of this quantity let us consider penetration probabilities for different partial waves in the case of a one-dimensional system (coupling to an internal system is neglected), Eq. (5). Under certain conditions, to be elaborated in the next subsection, we can approximate the ℓ dependence of the transmission probability at a given energy by simply shifting the energy (Balantekin *et al.*, 1983; Balantekin and Reimer, 1986):

$$T_\ell \simeq T_0\left[E-\frac{\ell(\ell+1)\hbar^2}{2\mu R^2(E)}\right], \tag{9}$$

where $\mu R^2(E)$ characterizes an effective moment of inertia. $R(E)$ was found to be a slowly varying function of energy, as depicted in Fig. 2. Consequently, in many applications, $R(E)$ is replaced by r_0, the position of the s-wave barrier, in Eq. (9). If many values of ℓ are important in the sum over partial-wave transmission probabilities in Eq. (1), we can approximate that sum with an integral over ℓ and, using Eq. (9), obtain (Balantekin *et al.*, 1983; Balantekin and Reimer, 1986)

$$E\sigma(E)=\pi R^2(E)\int_{-\infty}^{E} dE'\,T_0(E'). \tag{10}$$

It was found that Eq. (10) represents the experimental data for the total fusion cross section rather well (Balantekin and Reimer, 1986; Dasgupta *et al.*, 1991; Balantekin *et al.*, 1996). Differentiating Eq. (10) twice (Rowley *et al.*, 1991), one finds that the energy derivative of the s-wave transmission probability is approximately proportional to the second energy derivative of the quantity $E\sigma$ up to corrections coming from the energy dependence of $R(E)$:

$$\frac{dT_0(E)}{dE}\sim\frac{1}{\pi R^2(E)}\frac{d^2}{dE^2}[E\sigma(E)]+\mathcal{O}\left(\frac{dR}{dE}\right). \tag{11}$$

Since $R(E)$ is a slowly varying function of energy, the first term in Eq. (11) can be used to approximate the first derivative of the s-wave tunneling probability. For a completely classical system, T_0 is unity above the barrier and zero below; hence the quantity $dT_0(E)/dE$ will be a delta function peaked when E is equal to the barrier height, as shown in Fig. 3. Quantum mechanically this sharp peak is broadened as the transmission probability smoothly changes from zero at energies far below the barrier to unity at energies far above the barrier (see Fig. 3). Rowley *et al.* (1991) suggested that, if many channels are coupled to the translational motion, the quantity $dT_0(E)/dE$ is further broadened and can be taken to represent the "distributions of the barriers" due to the coupling to the extra degrees of freedom, as depicted in Fig. 4 for a two-channel case.

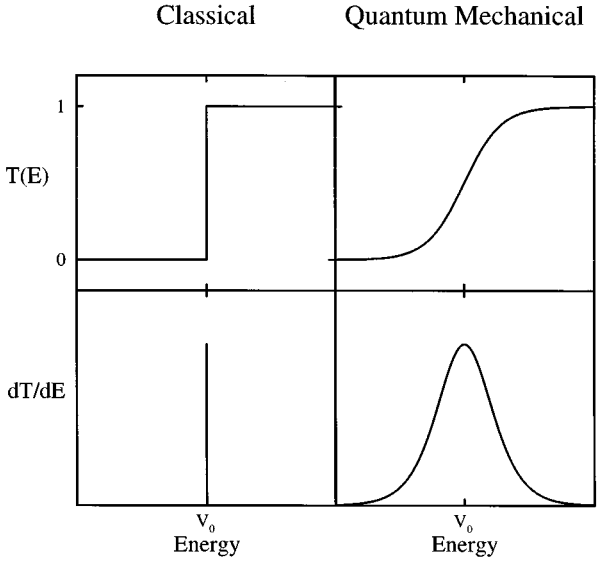

FIG. 3. Classical (on the left) and quantum-mechanical (on the right) transmission probabilities for a one-dimensional potential barrier.

Obviously one needs rather high-precision data to be able to calculate numerically the second derivative of the excitation function. Such high-quality data recently became available for a number of systems. As a specific example of the quality of recent data, Fig. 5 shows the measured cross section and the extracted associated barrier distribution for the ^{16}O+^{154}Sm system (Wei *et al.*, 1991; Leigh *et al.*, 1995).

Equations (9) and (10) [with the substitution $R(E)\rightarrow r_0$] can also be used to obtain a direct connection between the fusion cross section and the angular

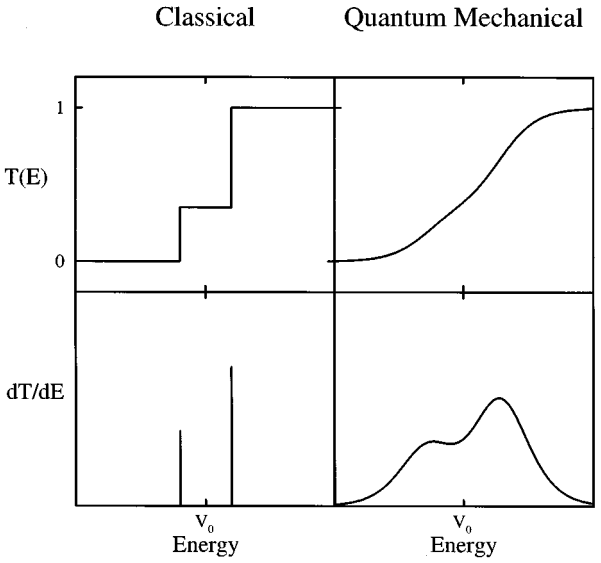

FIG. 4. Classical (on the left) and quantum-mechanical (on the right) transmission probabilities for a two-channel coupling. V_0 is the height of the one-dimensional potential barrier coupled to these channels.

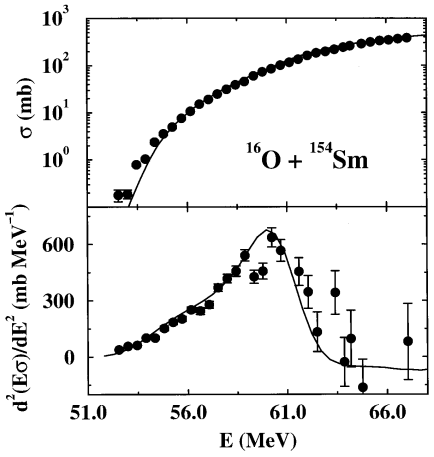

FIG. 5. Fusion cross section and barrier distribution for the ^{16}O+^{154}Sm system by Leigh *et al.* (1995).

momentum distribution (Sahm *et al.*, 1985; Ackermann, 1995):

$$T_\ell(E)=\frac{1}{\pi r_0^2}\left\{\frac{d[E'\sigma(E')]}{dE'}\right\}, \tag{12}$$

where

$$E'=E-(\hbar^2/2\mu r_0^2)\ell(\ell+1). \tag{13}$$

For energies well above the barrier, one can use the parabolic approximation of Eq. (7) for the potential barrier. Further approximating $R(E)$ by r_0 and inserting the penetration probability for the parabolic barrier, Eq. (8), in Eq. (10) one obtains an approximate expression for the cross section (Wong, 1973)

$$\sigma(E)=\frac{\hbar\Omega r_0^2}{2E}\log\left\{1+\exp\left[\frac{2\pi}{\hbar\Omega}(E-V_{B0})\right]\right\}. \tag{14}$$

In the classical limit, where $\Omega\rightarrow 0$ or $E\gg V_{B0}$, Eq. (14) reduces to the standard geometrical result

$$\sigma(E)=\pi r_0^2\left(1-\frac{V_{B0}}{E}\right). \tag{15}$$

D. Energy dependence of the effective radius

If one sets $R(E)=r_0$ in Eq. (9) for approximating the ℓ-wave penetrability by the s-wave penetrability at a shifted energy, one gets only the leading term in what is actually an infinite series expansion in $\Lambda=\ell(\ell+1)$. The next term in this expansion can easily be calculated. Let r_ℓ denote the position of the peak of the ℓ-wave barrier which satisfies

$$\left.\frac{\partial V_\ell(r)}{\partial r}\right|_{r=r_\ell}=0, \tag{16}$$

and

$$\left.\frac{\partial^2 V_\ell(r)}{\partial r^2}\right|_{r=r_\ell}<0. \tag{17}$$

Then the height of the barrier is given by $V_{B\ell}=V_\ell(r_\ell)$. We make the ansatz that the barrier position can be written as an infinite series,

$$r_\ell=r_0+c_1\Lambda+c_2\Lambda^2+\ldots, \tag{18}$$

where the c_i are constants. Expanding all functions in Eq. (16) consistently in powers of Λ, we find that the first coefficient is

$$c_1=-\frac{\hbar^2}{\mu\alpha r_0^3}, \tag{19}$$

where α is the curvature of the s-wave barrier

$$\alpha=-\left.\frac{\partial^2 V_0(r)}{\partial r^2}\right|_{r=r_0}. \tag{20}$$

Substituting the leading-order correction in the barrier position r_ℓ into Eq. (4), we find that to second order in Λ the ℓ-wave barrier height is given by

$$V_{B\ell}=V_{B0}+\frac{\hbar^2\Lambda}{2\mu r_0^2}+\frac{\hbar^4\Lambda^2}{2\mu^2\alpha r_0^6}. \tag{21}$$

Therefore an improved approximation for the ℓ dependence in the penetrability is given by

$$T_\ell(E)\approx T_0\left(E-\frac{\hbar^2\Lambda}{2\mu r_0^2}-\frac{\hbar^4\Lambda^2}{2\mu^2\alpha r_0^6}\right). \tag{22}$$

Comparing Eq. (21) with Eq. (6), we find that the energy-dependent effective radius can be expressed as (Balantekin *et al.*, 1996)

$$R^2(E)=r_0^2\left[1-\frac{4}{\alpha r_0^2}\frac{\int_0^E dE' T_0(E')(E-E')}{\int_0^E dE' T_0(E')}\right]. \tag{23}$$

This expression is useful in assessing whether the second derivative of the quantity $E\sigma$ will be usable as the distribution of barriers, since it gives an estimate of the terms neglected in Eq. (11). If we rewrite Eq. (11) including previously neglected terms,

$$\begin{aligned}\frac{dT_0(E)}{dE}=&\frac{1}{\pi R^2(E)}\frac{d^2}{dE^2}[E\sigma(E)]\\&-\frac{E\sigma(E)}{\pi R^4(E)}\frac{d^2}{dE^2}[R^2(E)]\\&-\frac{2T_0(E)}{R^2(E)}\frac{d}{dE}[R^2(E)],\end{aligned} \tag{24}$$

we see that a strong energy dependence of $R(E)$ would not only provide an overall multiplicative factor between the experimental observable $d^2(E\sigma)/dE^2$ and the true barrier distribution (i.e., dT_0/dE), but might also shift the position of various peaks in it and change the weights of these peaks. Equation (23) can be used to illustrate that such corrections are indeed small (Balantekin *et al.*, 1996). This is a useful consistency check even when channel-coupling effects yield a number of eigenbarriers (see Sec. III B) as Eq. (11) still needs to be satisfied for each one-dimensional eigenbarrier to be able to interpret experimentally determined $d^2(E\sigma)/dE^2$ as the distribution of barriers.

E. Inversion of the data

Using Abelian integrals (Cole and Good, 1978), one can show that for energies below the barrier

$$\int_E^{V_{B\ell}} dE'\,\frac{S_\ell(E')}{\sqrt{E'-E}}=\frac{\pi}{2}\sqrt{\frac{2\mu}{\hbar^2}}\int_{r_{1\ell}}^{r_{2\ell}} dr\left[V_0(r)+\frac{\hbar^2\ell(\ell+1)}{2\mu r^2}-E\right], \tag{25}$$

where $V_{B\ell}$ is the height of the ℓ-wave potential and $V_0(r)$ is the s-wave barrier. The energy derivative of the left-hand side of Eq. (25) can be integrated by parts to yield

$$\int_E^{V_{B\ell}} dE'\,\frac{\partial S_\ell(E')/\partial E'}{\sqrt{E'-E}}=-\frac{\pi}{2}\sqrt{\frac{2\mu}{\hbar^2}}\,(r_{2\ell}-r_{1\ell}), \tag{26}$$

which is used to find the barrier thickness (Balantekin *et al.*, 1983). Using Eqs. (5) and (9), one can relate the WKB penetration integral to the experimentally measured cross section as

$$S_0(E)=\frac{1}{2}\log\left(\left\{\frac{d}{dE}\left[\frac{E\sigma(E)}{\pi R^2(E)}\right]\right\}^{-1}-1\right). \tag{27}$$

Thus, if $R(E)$ is specified, the thickness of the barrier at a given energy is completely determined from the experimental data using Eqs. (26) and (27).

The potentials resulting from the analysis of Balantekin *et al.* (1983) for six systems are shown in Figure 6. For comparison, the point Coulomb potential and the phenomenologically determined potential of Krappe *et al.* (1979) are also shown. It should be emphasized that this inversion method assumes the existence of a single potential barrier. The thickness functions $t=r_{20}-r_{10}$ in Fig. 6, especially for the heavier systems, are inconsistent with the assumption of a single-valued one-dimensional local potential, clearly indicating the need for coupling to other degrees of freedom. This result was confirmed by the systematic study of Inui and Koonin (1984).

III. MULTIDIMENSIONAL QUANTUM TUNNELING IN NUCLEAR PHYSICS

A. Coupled-channels formalism

A standard theoretical approach to studying the effect of nuclear intrinsic degrees of freedom on the fusion cross section is to solve numerically the coupled-channels equations that determine the wave functions of the relative motion. For example, if one is interested in the effect of the excitation of the ground-state $K=0^+$ rotational band of the target nucleus, then each channel can be denoted by a set of indices (I,ℓ), where I and ℓ are the angular momentum of the rotational excited

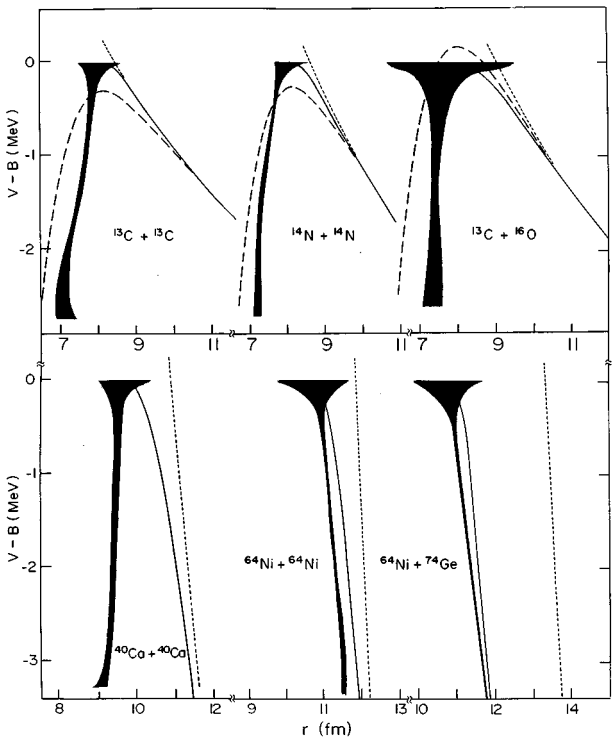

FIG. 6. Effective one-dimensional potential barriers from Balantekin *et al.* (1983). The outer turning points are determined from the phenomenological potential of Krappe *et al.* (1979) to fit the peak positions. The distance between the outer and inner turning points is the thickness function inverted from the data. The shaded region indicates the error envelope. The short-dashed line denotes the point Coulomb potential and the long-dashed line denotes the potential of Krappe *et al.* (1979).

states of the target nucleus and that of the relative motion, respectively. The coupled-channels equations then read

$$\left[-\frac{\hbar^2}{2\mu}\frac{d^2}{dr^2}+\frac{\hbar^2}{2\mu r^2}\ell_1(\ell_1+1)+V(r)-E_{I_1}\right]f_{I_1,\ell_1}(r)$$
$$+F_\lambda(r)\sum_{I_2,\ell_2}(-)^{J+\ell_2}i^{I_2+\ell_2-I_1-\ell_1}$$
$$\times\left[\frac{(2\ell_1+1)(2I_1+1)(2I_2+1)}{2\lambda+1}\right]^{1/2}\langle I_1 I_2 00|\lambda 0\rangle$$
$$\times\langle\ell_1\lambda 00|\ell_2 0\rangle\begin{Bmatrix}\ell_1 & I_1 & J\\ I_2 & \ell_2 & \lambda\end{Bmatrix}f_{I_2,\ell_2}(r)=0. \tag{28}$$

When the coupled-channels formalism is used to study direct reactions, the optical potential $V(r)$ contains an imaginary part in order to take into account the effect of intrinsic degrees of freedom other than the rotational excitation on the scattering. The multipolarity of the intrinsic excitation is $\lambda=2$ if we restrict the coupling to quadrupole deformations. The coupling form factor $F_\lambda(r)$ consists of Coulomb and nuclear parts,

$$F_\lambda(r)=F_C(r)+F_N(r). \tag{29}$$

If the coupling is restricted to quadrupole deformations, the Coulomb part is

$$F_C(r)=\frac{3}{\sqrt{20\pi}}\beta Z_1 Z_2 e^2\frac{R_c^2}{r^3}\quad(r\geq R_c)$$
$$=\frac{3}{\sqrt{20\pi}}\beta Z_1 Z_2 e^2\frac{r^2}{R_c^3}\quad(r<R_c) \tag{30}$$

and the nuclear part is

$$F_N(r)=-\sqrt{\frac{5}{4\pi}}\beta R_V\frac{dV_N}{dr}. \tag{31}$$

In most calculations the scale parameters R_c and R_V are taken to be $1.2A^{1/3}$. In the standard coupled-channels calculations, one solves Eq. (28) by imposing regular boundary condition at the origin. In contrast, in the study of heavy-ion fusion reactions, one takes the potential to be real and often solves Eq. (28) by imposing the incoming-wave boundary condition at some point inside the potential barrier to obtain S matrices. The fusion cross section is then obtained based on the unitarity relation as

$$\sigma=\frac{\pi}{k^2}\sum_\ell(2\ell+1)\left[1-\sum_a|S_a(\ell)|^2\right], \tag{32}$$

where the index a designates different scattering channels, which have been explicitly dealt with in the coupled-channels calculation. An advantage of the coupled-channels method is that one can try to analyze consistently heavy-ion fusion reactions and other scattering processes such as elastic scattering. Coupled-channels calculations for a number of systems exist in the literature (Dasso *et al.*, 1983; Lindsay and Rowley, 1984; Thompson *et al.*, 1985; Esbensen and Landowne, 1987; Stefanini *et al.*, 1990).

One can significantly reduce the number of channels in the coupled-channels calculations by ignoring the change of the centrifugal potential barrier due to the finite multipolarity of the nuclear intrinsic excitation (Takigawa and Ikeda, 1986; Esbensen *et al.*, 1987). This is called the no-Coriolis approximation, rotating-frame approximation, or isocentrifugal approximation (Gomez-Camacho and Johnson, 1988). A path-integral approach to the no-Coriolis approximation was given by Hagino *et al.* (1995).

If one further ignores the finite excitation energy of nuclear intrinsic motion, then one can completely decouple the coupled-channels equations into a set of single eigenchannel problems. These two approximations significantly simplify the numerical calculations and also give a clear physical understanding of the effect of channel coupling in terms of the distribution of potential barriers.

B. Simplified coupled-channels models

Under certain assumptions it is possible to simplify significantly the coupled-channels equations described in the previous section. We take the Hamiltonian to be

$$H=H_k+V_0(r)+H_0(\xi)+H_{\rm int}(\mathbf{r},\xi) \tag{33}$$

with the term H_k representing the kinetic energy

$$H_k = -\frac{\hbar^2}{2\mu}\nabla^2, \tag{34}$$

where $\mathbf{r}$ is the relative coordinate of the colliding nuclei and ξ represents any internal degrees of freedom of the target or the projectile. In this equation $V_0(r)$ is the bare potential and the term $H_0(\xi)$ represents the internal structure of the target or the projectile nucleus. Introducing the eigenstates of $H_0(\xi)$,

$$H_0|n\rangle = \epsilon_n|n\rangle, \tag{35}$$

and expanding the radial wave function as

$$\Psi(r) = \sum_n \chi_n(r)|n\rangle, \tag{36}$$

one reduces the time-independent Schroedinger equation to a set of coupled equations for the relative-motion wave functions χ_n,

$$\left[-\frac{\hbar^2}{2\mu}\frac{d^2}{dr^2} + V_{\not\subset}(r) - E\right]\chi_n(r) = -\sum_m [\epsilon_n\delta_{nm} + \langle n|H_{\rm int}(r,\xi)|m\rangle]\chi_m(r). \tag{37}$$

These equations are solved under the incoming-wave boundary conditions:

$$\chi_n(r) \to \left\{ \begin{array}{ll} \delta_{n0}\exp(-ik_n r) + \sqrt{\frac{k}{k_n}}\,R_n\exp(ik_n r), & r\to+\infty \\ \sqrt{\frac{k}{k_n}}\,T_n\exp(-ik_n r), & r\to r_{\rm min} \end{array} \right\}, \tag{38}$$

where $\hbar^2 k_n^2/2\mu = E - \epsilon_n$. The internal degrees of freedom are taken to be initially in their ground-state labeled by $n=0$ and the associated ground-state energy is set to be zero, $\epsilon_0 = 0$. In Eq. (38) the reflection and transmission coefficients in each channel are denoted by R_n and T_n, respectively.

Several groups (Dasso *et al.*, 1983a, 1983b; Broglia, Dasso, Landowne, and Pollarolo, 1983; Jacobs and Smilansky, 1983) studied various simplifying limits to emphasize salient physical features. Here we summarize the approach of Dasso *et al.* (1983a). They assumed that the coupling interaction factors into a relative part, $F(r)$, and an intrinsic part, $G(\xi)$:

$$M_{nm} \equiv \epsilon_n\delta_{nm} + \langle n|H_{\rm int}(r,\xi)|m\rangle = \epsilon_n\delta_{nm} + F(r)\langle n|G(\xi)|m\rangle, \tag{39}$$

and that the form factor $F(r)$ is a constant [taken by Dasso *et al.* (1983b) to be the value of $F(r)$ at the barrier position]. Under these approximations the coupled-channel equations decouple to give

$$\left[-\frac{\hbar^2}{2\mu}\frac{d^2}{dr^2} + V_{\not\subset}(r) + \lambda_n - E\right]\left[\sum_m U_{nm}\chi_m(r)\right] = 0, \tag{40}$$

where U_{nm} is the unitary matrix that diagonalizes the coupling matrix M_{nm} to give a set of eigenvalues λ_n. Equation (40) indicates that the effect of the coupling is to replace the original barrier by a set of eigenbarriers $V_{\not\subset}(r) + \lambda_n$. The transmission probability calculated in the incoming-wave boundary conditions is given by

$$T_{\not\subset}(E) = \sum_n |U_{n0}|^2 T_{\not\subset}(E - \lambda_n), \tag{41}$$

where $T_{\not\subset}(E-\lambda_n)$ is the transmission probabilities calculated at shifted energies $E-\lambda_n$.

Even though the constant-coupling approach would overpredict the transmission probability, it can nevertheless be used to get a qualitative understanding of the dependence of the fusion cross section on various physical quantities. For example, one can study coupling to a harmonic mode with a finite Q value using the model Hamiltonian

$$M = \pi^2/2D + \frac{1}{2}C\xi^2 + F_0\xi, \tag{42}$$

yielding

$$M_{mn} = -nQ\,\delta_{mn} + F(\sqrt{n}\,\delta_{n,m+1} + \sqrt{n+1}\,\delta_{n,m-1}), \tag{43}$$

where $-Q = \hbar\sqrt{C/D}$ is the excitation energy, $F = F_0\sqrt{|Q|/2C}$ measures the total strength of the coupling, and the eigenvalues are

$$\lambda_n = n|Q| - F^2/|Q|. \tag{44}$$

The total transmission probability can easily be calculated to be

$$T_{\rm cc}(E) = \sum_{n=0}^{\infty} (F^{2n}/Q^{2n}n!)\exp(-F^2/Q^2) \times T(E - n|Q| + F^2/|Q|). \tag{45}$$

In the special case of a two-channel problem the matrix

$$M = \begin{pmatrix} 0 & F \\ F & -Q \end{pmatrix} \tag{46}$$

has eigenvalues

$$\lambda_{\pm}=\frac{1}{2}(-Q\pm\sqrt{Q^2+4F^2}), \tag{47}$$

with the corresponding weight factors

$$U_{\pm}^2=\frac{2F^2}{4F^2+Q^2\mp Q\sqrt{4F^2+Q^2}}. \tag{48}$$

Note that for $F/|Q|<1$ the lowest effective barrier carries the largest weight for negative Q, while the situation is reversed for positive Q (see Sec. V.B).

Tanimura *et al.* (1985) pointed out that the constant-coupling approximation can overestimate low-energy fusion rates where the coupling effects are strong and the associated form factors are rapidly varying. Dasso and Landowne (1987a) extended their model for strong-coupling cases. They diagonalized the coupled intrinsic system in the barrier region to obtain the eigenstates $|\gamma(r)\rangle$ and the eigenvalues $\lambda_\gamma(r)$ as functions of r to obtain the total transmission probability

$$T_{\rm scc}(E)=\sum_\gamma |\langle\gamma(R)|0\rangle|^2 T_\gamma[E,V(r)+\lambda_\gamma(r)], \tag{49}$$

where $T_\gamma[E,V(r)+\lambda_\gamma(r)]$ is the penetration probability for the potential $V(r)+\lambda_\gamma(r)$. The weighing factors are fixed at a chosen radius R, which might be the position of the unperturbed barrier or the average position of the eigenbarriers. Two coupled-channels codes, simplified in this manner, are available in the literature: CCFUS (Dasso and Landowne, 1987b) and CCDEF (Fernandez-Niello *et al.*, 1989). Both of them treat the vibrational coupling in the constant-coupling approximation. The latter takes into account projectile and target deformations within the sudden approximation and treats coupling to the transfer channels with a constant form factor.

In CCFUS the basis states included are the ground state $|0\rangle$, the quadrupole one-phonon state $b_2^\dagger|0\rangle$, the octupole one-phonon state $b_3^\dagger|0\rangle$, and the product two-phonon state $b_2^\dagger b_3^\dagger|0\rangle$. The resulting matrix to be diagonalized to yield the eigenchannels is

$$M=\begin{pmatrix} 0 & F_2(r) & F_3(r) & 0 \\ F_2(r) & \epsilon_2 & 0 & F_3(r) \\ F_3(r) & 0 & \epsilon_3 & F_2(r) \\ 0 & F_3(r) & F_2(r) & \epsilon_2+\epsilon_3 \end{pmatrix}. \tag{50}$$

In CCFUS the double-phonon states $(b_2^\dagger)^2|0\rangle$ and $(b_3^\dagger)^2|0\rangle$ are not included for mathematical simplification. The eigenvalues of the matrix in Eq. (50) can be written as the sums of the eigenvalues of the two 2×2 matrices, which represent the coupling of the single one-phonon states, i.e.,

$$M_2=\begin{pmatrix} 0 & F_2(r) \\ F_2(r) & \epsilon_2 \end{pmatrix} \tag{51}$$

and

$$M_3=\begin{pmatrix} 0 & F_3(r) \\ F_3(r) & \epsilon_3 \end{pmatrix}. \tag{52}$$

If the matrix of Eq. (50) also included the double-phonon states $(b_2^\dagger)^2|0\rangle$ and $(b_3^\dagger)^2|0\rangle$, such a simple relationship between eigenvalues of the 4×4 and 2×2 matrices would not be possible. CCFUS provides two options: the matrices of Eqs. (51) and (52) are either diagonalized by replacing the form factors $F_2(r)$ and $F_3(r)$ with their values at the location of the bare potential barrier or diagonalized for all values of r. In the latter case only the weight factors, not the eigenvalues, are evaluated at the position of the bare barrier. The transmission coefficients for each eigenbarrier are calculated using the Wong formula, Eq. (14).

The approach of CCFUS can be generalized to incorporate n different phonons by including the ground state, n one-phonon states, $n(n-1)/2$ two-phonon states (i.e., not those states in which the same phonon appears more than once), $n(n-1)(n-2)/3!$ three-phonon states, etc. to obtain a total number of

$$1+n+\frac{n(n-1)}{2!}+\frac{n(n-1)(n-2)}{3!}+\frac{n(n-1)(n-2)(n-3)}{4!}+\cdots=2^n \tag{53}$$

states. Since no phonon appears more than once, the eigenvalues of the resulting $2^n\times2^n$ matrix can be written as appropriate combinations of the eigenvalues of n 2×2 matrices. Even though the approach of CCFUS provides an elegant mathematical solution to the matrix diagonalization problem, it ignores all the states in which the same phonon appears more than once, e.g., the double-phonon states. Dasgupta *et al.* (1992) and Kruppa *et al.* (1993) pointed out that in some cases the coupling of a state like $(b_i^\dagger)^2|0\rangle$ to the ground state can be stronger than the coupling of a state like $b_i^\dagger b_j^\dagger|0\rangle$, $i\neq j$. Kruppa *et al.* (1993) considered quadrupole and octupole phonons, but included their double-phonon states as well, diagonalizing the resulting 6×6 matrix. Dasgupta *et al.* (1992) excluded all multiple-phonon states, so for n different types of phonons they numerically diagonalized a $(n+1)\times(n+1)$ matrix instead of analytically diagonalizing a $2^n\times2^n$ matrix. The resulting simplified coupled-channels code is named CCMOD (Dasgupta *et al.*, 1992). In CCMOD the weight factors are calculated at the position of the bare barrier, but the energy dependence of $R(E)$ in Eq. (9) is taken into account using the prescription of Rowley *et al.* (1989). Eigenchannel cross sections are again calculated using the Wong formula.

Many experimentalist use these simplified coupled-channel codes. When using them it is important to remember the approximations discussed in the previous paragraphs. Some of these approximations (constant coupling, Wong's formula) lead to an overestimate of the cross section. Some of the ignored couplings (e.g., the double-phonon states) may be very important for the dynamics of the analyzed system. We therefore recommend using these codes only for a qualitative under-

standing of the data and strongly encourage authors to use full coupled-channel codes for any quantitative description.

Finally one should point out that in the limit in which the intrinsic energies are small compared to the coupling interaction one can approximate Eq. (39),

$$M_{nm} \sim F(r)\langle n|G(\xi)|m\rangle. \tag{54}$$

In this case it is not necessary to require that the coupling be constant. The transformation amplitude between the ground state and the eigenchannels labeled by ξ is the ground-state wave function yielding the transmission probability

$$T_{\text{total}} = \int d\xi |\psi(\xi)|^2 T[E, V(r)+F(r)G(\xi)], \tag{55}$$

where $T[E,V(r)+F(r)G(\xi)]$ is the transmission probability for the potential $V(r)+F(r)G(\xi)$ calculated at energy E.

C. Path-integral approach

An alternative formulation of multidimensional quantum tunneling is given by the path-integral formalism (Balantekin and Takigawa, 1985). For the Hamiltonian given in Eq. (33) the propagator to go from an initial state characterized by relative radial coordinate r_i (the magnitude of **r**) and internal quantum numbers n_i to a final state characterized by the radial position r_f and the internal quantum numbers n_f may be written as

$$K(r_f,n_f,T;r_i,n_i,0) = \int \mathcal{D}[r(t)] e^{iS(r,T)/\hbar} W_{n_f n_i}[r(t),T], \tag{56}$$

where $S(r,T)$ is the action for the translational motion and $W_{n_f n_i}$ is the propagator for the internal system along a given path of the translational motion:

$$W_{n_f n_i}(r,T) = \langle n_f|\hat{U}_{\text{int}}[r(t),T]|n_i\rangle. \tag{57}$$

$\hat{U}_{\text{int}}$ satisfies the differential equation

$$i\hbar \frac{\partial \hat{U}_{\text{int}}}{\partial t} = (H_0 + H_{\text{int}})\hat{U}_{\text{int}}, \tag{58}$$

$$\hat{U}_{\text{int}}(t=0) = 1. \tag{59}$$

We want to consider the case in which r_i and r_f are on opposite sides of the barrier. In the limit when the initial and final states are far away from the barrier, the transition amplitude is given by the S-matrix element, which can be expressed in terms of the propagator as (Balantekin and Takigawa, 1985)

$$S_{n_f,n_i}(E) = -\frac{1}{i\hbar} \lim_{\substack{r_i\to\infty \\ r_f\to-\infty}} \left(\frac{p_i p_f}{\mu^2}\right)^{1/2} \exp\left[\frac{i}{\hbar}(p_f r_f - p_i r_i)\right] \times \int_0^\infty dT e^{+iET/\hbar} K(r_f,n_f,T;r_i,n_i,0), \tag{60}$$

where p_i and p_f are the classical momenta associated with r_i and r_f. In heavy-ion fusion we are interested in the transition probability in which the internal system emerges in any final state. For the ℓth partial wave, this is

$$T_\ell(E) = \sum_{n_f} |S_{n_f,n_i}(E)|^2, \tag{61}$$

which becomes, upon substituting Eqs. (57) and (60),

$$T_\ell(E) = \lim_{\substack{r_i\to\infty \\ r_f\to-\infty}} \left(\frac{p_i p_f}{\mu^2}\right) \int_0^\infty dT \exp\left(\frac{i}{\hbar}ET\right) \int_0^\infty d\tilde{T} \times \exp\left(-\frac{i}{\hbar}E\tilde{T}\right) \int \mathcal{D}[r(t)] \int \mathcal{D}[\tilde{r}(\tilde{t})] \times \exp\left\{\frac{i}{\hbar}[S(r,T) - S(\tilde{r},\tilde{T})]\right\} \times \rho_M[\tilde{r}(\tilde{t}),\tilde{T};r(t),T]. \tag{62}$$

Here we have assumed that the energy dissipated to the internal system is small compared to the total energy and we have taken p_f outside the sum over final states. We identified the two-time influence functional as

$$\rho_M[\tilde{r}(\tilde{t}),\tilde{T};r(t),T] = \sum_{n_f} W^*_{n_f,n_i}[\tilde{r}(\tilde{t});\tilde{T},0] \times W_{n_f,n_i}[r(t);T,0]. \tag{63}$$

Using the completeness of final states, we can simplify this expression to

$$\rho_M[\tilde{r}(\tilde{t}),\tilde{T};r(t),T] = \langle n_i|\hat{U}^\dagger_{\text{int}}[\tilde{r}(\tilde{t}),\tilde{T}] \times \hat{U}_{\text{int}}[r(t),T]|n_i\rangle. \tag{64}$$

Equation (64) shows the utility of the influence functional method when the internal system has symmetry properties. If the Hamiltonian in Eq. (58) has a dynamical or spectrum-generating symmetry, i.e., if it can be written in terms of the Casimir operators and generators of a given Lie algebra, then the solution of Eq. (58) is an element of the corresponding Lie group (Balantekin and Takigawa, 1985). Consequently the two-time influence functional of Eq. (64) is simply a diagonal group matrix element for the lowest-weight state and it can be evaluated using standard group-theoretical methods. This is exactly the reason why the path-integral method is very convenient when the internal structure is represented by an algebraic model such as the interacting boson model.

Two-time influence functionals can be calculated exactly for only a limited number of systems. One of these is a harmonic oscillator, linearly coupled to the translational motion. In this case the Hamiltonian is

$$H = -\frac{\hbar^2}{2\mu_0}\frac{\partial^2}{\partial r^2} + V_0(r) + (a^\dagger a + \tfrac{1}{2})\hbar\omega + \alpha_0 f(r)(a+a^\dagger), \tag{65}$$

where μ_0 is the bare mass of the macroscopic motion and $V_0(r)$ is the bare potential. The $a^\dagger(a)$, ω, m, and

$f(r)$ are the creation (annihilation) operators of the oscillator quanta, the frequency and the mass parameter of the oscillator, and the coupling form factor, respectively. The quantity $\alpha_0=(\hbar/2m\omega)^{1/2}$ represents the amplitude of the zero-point motion of the harmonic oscillator. The two-time influence functional ρ_M reflects the effects of coupling to the harmonic oscillator and is given by

$$\rho_M[\tilde{r}(\tilde{t}),\tilde{T};r(t),T]=\exp\left[-\frac{i}{2}\omega(T-\tilde{T})\right]\times\exp\left[-\frac{\alpha_0^2}{\hbar^2}(y_1+y_2+y_3)\right] \quad (66)$$

with

$$y_1=\int_0^T dt\int_0^t ds f[r(t)]f[r(s)]e^{-i\omega(t-s)},$$
$$y_2=\int_0^{\tilde{T}} d\tilde{t}\int_0^{\tilde{t}} d\tilde{s} f[\tilde{r}(\tilde{t})]f[\tilde{r}(\tilde{s})]e^{i\omega(\tilde{t}-\tilde{s})},$$
$$y_3=-e^{i\omega(\tilde{T}-T)}\int_0^T dt f[r(t)]e^{i\omega t}\int_0^{\tilde{T}} d\tilde{t} f[\tilde{r}(\tilde{t})]e^{-i\omega\tilde{t}}. \quad (67)$$

An exact calculation of the influence functional is possible in this case because of the symmetry of the Hamiltonian under the Heisenberg-Weyl algebra.

D. Adiabatic and sudden tunneling

We can discuss the effects of couplings between nuclear structure and translational motion in two limiting cases. The first case is the sudden limit in which the energy levels of the internal system are degenerate. The second case is the adiabatic limit in which the energy of the first excited state of the system is very large so that the internal system emerges in the ground state at the other side of the barrier.

Several examples are worked out explicitly by Balantekin and Takigawa (1985), to which article the reader is referred for further details. It can be shown that, in the sudden limit, the total transmission probability is given by an integral of transmission probabilities for a fixed value of the internal coordinate, with the weight of the integration given by the distribution of the internal coordinate in its ground state. For example, for the linearly coupled harmonic oscillator, as the excitation energy gets smaller, $\omega\to 0$, the influence functional of Eq. (66) takes the form

$$\rho_M[\tilde{r}(\tilde{t}),\tilde{T};r(t),T]=\exp\left(-\frac{\alpha_0^2}{2\hbar^2}\left\{\int_0^T dt f[r(t)]-\int_0^{\tilde{T}} d\tilde{t} f[\tilde{r}(\tilde{t})]\right\}^2\right). \quad (68)$$

Using the integral

$$\int_{-\infty}^{\infty} dx e^{-(ax^2+bx)}=\sqrt{\frac{\pi}{a}}\,e^{b^2/4a} \quad (69)$$

we can rewrite the influence functional as

$$\rho_M[\tilde{r}(\tilde{t}),\tilde{T};r(t),T]=\rho_S[\tilde{r}(\tilde{t}),\tilde{T};r(t),T]\equiv\frac{1}{\alpha_0\sqrt{2\pi}}\int_{-\infty}^{\infty} d\alpha e^{-(\alpha/\alpha_0)^2/2}\times\exp\left(-\frac{i\alpha}{\hbar}\left\{\int_0^T dt f[r(t)]-\int_0^{\tilde{T}} d\tilde{t} f[\tilde{r}(\tilde{t})]\right\}\right) \quad (70)$$

where the lower suffix s stands for sudden tunneling. Inserting this expression into Eq. (62), one obtains

$$T(E)=\frac{1}{\sqrt{2\pi}}\int_{-\infty}^{+\infty} dx e^{-x^2/2}T_0[E,V_0(r)+x\alpha_0 f(r)], \quad (71)$$

where $T_0[E,V_0(r)+x\alpha f(r)]$ is the probability of tunneling through the one-dimensional barrier $V_0(r)+x\alpha f(r)$ at energy E. This expression is known as the zero-point motion formula and was first derived by Esbensen (1981). This result can also be derived either using the coupled-channels formalism (cf. Sec. III.B) or using Green's functions (Takigawa *et al.*, 1992). Similarly, if the translational motion couples to a very slow rotational motion through a coupling Hamiltonian given by

$$H_{\rm int}=\sqrt{\frac{5}{4\pi}}\,\beta P_2(\cos\theta)f(r), \quad (72)$$

then the net tunneling probability is obtained by first calculating the tunneling probability for a fixed orientation of the principal axis of the deformed nucleus, and then taking an average over all orientations,

$$T(E)=\int_0^1 d\cos\theta T_0\left[E,V_0(r)+\sqrt{\frac{5}{4\pi}}\,\beta P_2(\cos\theta)f(r)\right]. \quad (73)$$

This formula was first derived by Chase *et al.* (1958) in the study of scattering of rotational nuclei in the sudden approximation. Systematics of the fusion cross sections of ^{16}O with a series of Sm isotopes, ranging from vibrational to rotational, was first given by Stokstad and Gross (1981) using Eq. (73).

In actual calculations, both vibrational and rotational excitations are truncated at finite excited states. In these cases, the Hermite and the Gauss integrals in Eqs. (71) and (73) are replaced by the Hermite and the Gauss quadratures, respectively (Nagarajan *et al.*, 1986). Zero-point motion formulas then have a simple geometric interpretation: In this approximation fusion of a deformed nucleus with a finite number (N) of levels can be described by sampling N orientations with their respective weights:

$$\sigma(E)=\sum_{i=1}^{N}\omega_i\sigma[E,V_0(R)+\lambda_i f(r)], \quad (74)$$

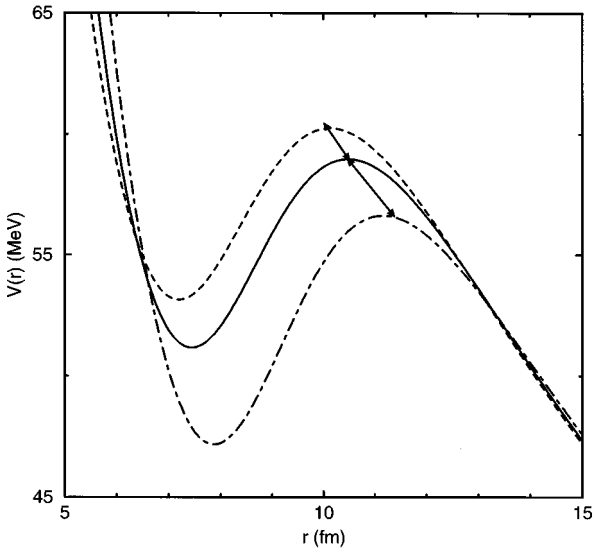

FIG. 7. Illustration of the geometric interpretation of the sudden approximation. The solid curve is the total potential for the $^{16}O+^{154}Sm$ system when the projectile is taken to be spherical. The dashed ($\lambda=-0.327$) and dot-dashed ($\lambda=+0.613$) curves are potentials for the two-level approximation for the target with $\beta=0.25$. The arrows show the shifts predicted for the barrier peaks (Balantekin *et al.*, 1996).

where $\Sigma_{i=1}^{N}\omega_i=1$. For example, in a two-level system, the orientations $\theta_1=70.12°$ and $\theta_2=30.55°$ contribute with weight factors $\omega_1=0.652$ and $\omega_1=0.348$, respectively, as illustrated in Fig. 7.

When both target and projectile are heavy and deformed, one needs a model describing macroscopic potential-energy surfaces for arbitrarily oriented, deformed heavy ions. Such a model describing completely general configurations of two separated nuclei is given by Möller and Iwamoto (1994).

In the adiabatic limit, i.e., that of slow tunneling, one can introduce (Balantekin and Takigawa, 1985) an Ω/ω expansion, ω and Ω being the frequencies of the internal motion and the tunneling barrier, respectively. In this limit the effects of coupling to internal degrees of freedom can be represented in terms of an energy-independent potential renormalization (Balantekin and Takigawa, 1985; Müller and Takigawa, 1987),

$$V_0(r)\rightarrow V_{ad}=V_0(r)-\alpha_0^2 f^2(r)/\hbar\omega, \tag{75}$$

and a mass renormalization (Takigawa *et al.*, 1994),

$$\mu_0\rightarrow\mu_{\rm ad}=\mu_0+2\frac{\alpha_0^2}{\hbar\omega}\frac{1}{\omega^2}\left(\frac{df}{dr}\right)^2. \tag{76}$$

This limit is very closely related to the situation investigated by Caldeira and Leggett (1983) in their study of multidimensional quantum tunneling. In the Caldeira-Leggett formalism the term that renormalizes the potential in Eq. (75) is added to the Lagrangian as a counterterm. Note that the correction term to the potential is the well-known polarization potential, and the correction term to the mass is the cranking mass. Hence appropriate generalizations of Eqs. (75) and (76) hold not only for a linearly coupled oscillator, but for any system (Takigawa *et al.*, 1994). Effects of the polarization potential on the subbarrier fusion cross section were elucidated by Tanimura *et al.* (1985).

Typically an adiabatic barrier alone overpredicts the transmission probability. We can demonstrate this for the constant-coupling case ($\mu_{\rm ad}=\mu_0$) using the exact coupled-channels result of Eq. (45),

$$T_{\rm cc}(E)=\sum_{n=0}^{\infty}\frac{1}{n!}\left(\frac{\alpha_0 f}{\hbar\omega}\right)^{2n}\exp[-\alpha_0^2 f^2/(\hbar\omega)^2]\times T\left(E-n\hbar\omega+\frac{\alpha_0^2 f^2}{\hbar\omega}\right). \tag{77}$$

Inserting the inequality

$$T\left(E-n\hbar\omega+\frac{\alpha_0^2 f^2}{\hbar\omega}\right)\leq T\left(E+\frac{\alpha_0^2 f^2}{\hbar\omega}\right) \tag{78}$$

into Eq. (77), we get

$$T_{\rm cc}(E)\leq T_{\rm adiabatic}(E). \tag{79}$$

We should emphasize that in the adiabatic limit both the potential and the mass renormalization should be considered together. Many authors refer to using only the adiabatic potential as the adiabatic limit. While for constant coupling it is true that $\mu_{\rm ad}=\mu_0$, in most cases of interest to nuclear fusion the coupling form factors rapidly change near the barrier, and the difference between the adiabatic mass and the bare mass can get very large. In these cases, using the adiabatic correction to the mass in addition to the adiabatic potential, even though the former is in the next order in $1/\omega$ as compared to the latter, can significantly reduce the transmission probability to values below the exact coupled-channels result (Takigawa *et al.*, 1994).

Adiabatic and sudden approximations are very useful for obtaining analytical results which provide a conceptual framework for understanding the fusion process. For deformed nuclei, in which the excitation energies are very low, sudden approximation provides a reasonably good description of the data. In rotation-vibration coupling, sudden approximation can be utilized to reduce the size of the channel coupling.

If the excitation energies of the internal system are large, the sudden approximation tends to overestimate the tunneling probability at energies well below the barrier. Indeed Esbensen *et al.* (1983) showed that, at energies below the barrier, sudden approximation provides an upper limit to the tunneling probability. Using the path-integral approach Hagino, Takigawa, Bennett, and Brink (1995) showed that, for a nearly degenerate system, the finite excitation energy leads to a multiplicative dissipation factor which reduces the barrier penetrability estimated in the sudden limit. This latter result also provides a good example of the utility of the path-integral method. As we mentioned earlier, for Hamiltonians written in terms of the generators of a Lie algebra, the path-integral approach is especially convenient, as integrals over paths become integrals over the group mani-

fold and thus are amenable to the standard group-theoretical techniques. An example of this is the treatment of nuclear structure effects in subbarrier fusion with the interacting boson model discussed in Sec. IV. Finally coupled-channel techniques are not practical as the number of channels gets very large, e.g., for tunneling problems at finite temperature. On the other hand, for finite-temperature problems, path-integral techniques can easily be applied [see, for example, Abe and Takigawa (1988) where particle decay from a hot compound nucleus is investigated and the thermal fluctuation of the nuclear surface is shown to amplify the dynamic effect].

E. Intermediate cases—dynamic norm method

In the intermediate cases between sudden and adiabatic tunneling, the effects of the environment are not straightforward to illustrate in simple physical terms. The dynamic norm method (Brink, 1985b; Takigawa, Hagino, and Abe, 1995) is a technique introduced to give an intuitive understanding of the effects of the environment in the intermediate cases. One defines the adiabatic basis by

$$\{H_0(\xi)+H_{\rm int}[\xi,r(t)]\}\phi_n[r(t),\xi] \equiv h[r(t),\xi]\phi_n[r(t),\xi]=\epsilon_n[r(t)]\phi_n[r(t),\xi]. \quad (80)$$

In the same spirit as the WKB approximation for a potential model, for the total wave function one can take the ansatz

$$\Psi(r,\xi)=\Phi(r,\xi)\left(\frac{dW}{dr}\right)^{-1/2} e^{i\epsilon W(r)/\hbar}. \quad (81)$$

Here the parameter ϵ is 1 and -1 in classically allowed and in classically forbidden regions, respectively, and the action obeys the Hamilton-Jacobi equation,

$$\frac{\epsilon^2}{2\mu_0}\left(\frac{dW}{dr}\right)^2+V_{ad}(r)=E \quad (82)$$

where V_{ad} is the adiabatic potential defined by

$$V_{ad}(r)=V_0(R)+\epsilon_0(r). \quad (83)$$

One can then derive an approximate expression in which the net tunneling probability is given by the product of the tunneling probability through the adiabatic potential barrier and a multiplicative factor, which represents the nonadiabatic effect of the intrinsic degrees of freedom,

$$T=T_0(E,V_{ad})\cdot\mathcal{N}(\tau_b),$$

$$\mathcal{N}(\tau)=\int d\xi|\Phi[r(\tau),\xi]|^2. \quad (84)$$

Here τ_b is the time when the tunneling process is completed. Note that in this approximation the transmission probability is calculated with the bare mass, not the renormalized mass of Eq. (76). One can easily show that $\mathcal{N}\leqslant 1$. This means that the transmission probability calculated with the adiabatic potential is always greater than the actual transmission probability. The deviation of $\mathcal{N}$ from 1 gives the measure of non-adiabaticity of the tunneling process.

One way to determine the dynamic norm factor $\mathcal{N}$ is to first expand $\Phi(r,\xi)$ in the basis of the adiabatic states $\phi_n[r(\tau),\xi]$,

$$\Phi(r,\xi)=\sum_n a_n(\tau)\cdot\phi_n[r(\tau),\xi], \quad (85)$$

and then determine the expansion coefficients a_n by solving the coupled-channels equations

$$\dot{a}_n(\tau)-\dot{r}(\tau)\sum_{m\neq n} a_m(\tau)\frac{1}{\epsilon_n[r(\tau)]-\epsilon_m[r(\tau)]} \times\langle\phi_n|\frac{\partial\tilde{h}}{\partial r}|\phi_m\rangle=-\frac{1}{\hbar}\tilde{\epsilon}_n[r(\tau)]a_n(\tau) \quad (86)$$

with $\tilde{\epsilon}_n=\epsilon_n[r(\tau)]-\epsilon_0[r(\tau)]$. Note that Eq. (86) correctly describes a classically forbidden region. One needs to modify it with ϵ in order to describe a classically allowed region. As an example, consider a linearly coupled oscillator with the coupling form factor given by $f(r)=cr$. Assuming that the tunneling path is given by $t(\tau)=R_0\sin(\Omega\tau)$, R_0 being the length of the tunneling region, we obtain

$$\mathcal{N}(\tau_b)\sim\exp\left[-\frac{\pi}{2}\left(\frac{c\alpha_0R_0}{\hbar\omega}\right)^2\frac{\Omega}{\omega}\right]. \quad (87)$$

Equation (87) shows that the adiabaticity of the tunneling process is governed not only by a parameter Ω/ω, but also by the coupling strength and the length of the tunneling region. Takigawa, Hagino, and Abe (1995) applied the dynamic norm method to spontaneous fission of ^{234}U.

IV. DESCRIPTION OF NUCLEAR STRUCTURE EFFECTS BY THE INTERACTING BOSON MODEL

An algebraic nuclear structure model significantly simplifies evaluation of the path integral. The interacting boson model (IBM) of Arima and Iachello (Iachello and Arima, 1987) is one such model, which has been successfully employed to describe the properties of low-lying collective states in medium-heavy nuclei. In this section, attempts to use the IBM in describing nuclear structure effects on fusion are reviewed. The path-integral formulation of this problem, as sketched in the next section, requires analytic solutions for the nuclear wave functions. In the first attempt to use the IBM to describe nuclear structure effects in subbarrier fusion, the SU(3) limit of the IBM was employed (Balantekin *et al.*, 1991). However, the SU(3) limit corresponds to a rigid nucleus with a particular quadrupole deformation and no hexadecapole deformation, a situation not realized in most deformed nuclei. Thus analytic solutions away from the limiting symmetries of the IBM are needed for realistic calculations of subbarrier fusion cross sections.

In a parallel development, a $1/N$ expansion was investigated (Kuyucak and Morrison, 1988, 1989a, 1989b) for the IBM which provided analytic solutions for a general Hamiltonian with arbitrary kinds of bosons. This technique proved useful in a variety of nuclear structure problems in which direct numerical calculations are prohibitively difficult. Later it was applied to medium-energy proton scattering from collective nuclei (Kuyucak and Morrison, 1993) in the Glauber approximation, generalizing the earlier work done using the SU(3) limit (Ginocchio *et al.*, 1986). Using the $1/N$ expansion technique in the path-integral formulation of the fusion problem (Balantekin *et al.*, 1992) makes it possible to get away from the three symmetry limits of the IBM. In particular, arbitrary quadrupole and hexadecapole couplings can be introduced.

A. Linear coupling

We take $H_{\rm int}$ in Eq. (33) to be of the form of the most general one-body transition operator for the interacting boson model,

$$H_{\rm int}=\sum_{kjl}\ \alpha_{kjl}(r)[b_j^{\dagger}\tilde{b}_l]^{(k)}\cdot Y^{(k)}(\hat{\mathbf{r}}), \tag{88}$$

where the boson operators are denoted by b_l and $b_j^{\dagger}$. The k sum runs over $k=2,4,\ldots,2\ell_{\max}$. Odd values of k are excluded as a consequence of the reflection symmetry of the nuclear shape, and the $k=0$ term is already included in the bare potential $V_0(r)$. The form factors $\alpha_{kjl}(r)$ represent the spatial dependence of the coupling between the intrinsic and translational motions. The interaction term given in Eq. (88) is an element of the SU(6) algebra for the original form of the interacting boson model with s and d bosons and is an element of the SU(15) algebra when g bosons are included as well (Iachello and Arima, 1987).

To simplify the calculation of the influence functional, we use the no-Coriolis approximation. We first perform a rotation at each instant to a frame in which the z axis points along the direction of relative motion. Neglecting the resulting centrifugal and Coriolis terms in this rotating frame is equivalent to ignoring the angular dependence of the original Hamiltonian. In this approximation, the coupling form factors become independent of ℓ and only $m=0$ magnetic substates of the target are excited (Takigawa and Ikeda, 1986; Esbensen *et al.*, 1987; Tanimura, 1987). For heavy systems the neglected centrifugal and Coriolis forces are small. We take the scattering to be in the x-y plane. Then, making a rotation through the Euler angles $\hat{\mathbf{b}}=(\phi,\pi/2,0)$, we can write the full Hamiltonian as the rotation of a simpler Hamiltonian depending only on the magnitude of $\mathbf{r}$,

$$H=R(\hat{\mathbf{b}})H^{(0)}(r)R^{\dagger}(\hat{\mathbf{b}}). \tag{89}$$

Since in Eq. (33) H_0 and $H_t=H_k+V_0(r)$ are rotationally invariant, $H_{\rm int}$ is the only term whose form is affected by the transformation. Hence we introduce the rotated interaction Hamiltonian $H_{\rm int}^{(0)}(r)$, given by

$$H_{\rm int}=R(\hat{\mathbf{b}})H_{\rm int}^{(0)}(r)R^{\dagger}(\hat{\mathbf{b}}), \tag{90}$$

$$H_{\rm int}^{(0)}(r)=\sum_{jlm}\ \phi_{jlm}(r)b_{jm}^{\dagger}b_{lm}\,, \tag{91}$$

$$\phi_{jlm}(r)=(-1)^m\sum_k\ \sqrt{\frac{2k+1}{4\pi}}\times\langle jml-m|k0\rangle\alpha_{kjl}(r). \tag{92}$$

If we assume now that the form factors $\alpha_{kjl}(r)$ are all proportional to the same function of r, then the Hamiltonian $H_{\rm int}^{(0)}$ commutes with itself at different times and hence we can write the two-time influence functional as

$$\rho_M=\left\langle n_i\left|\exp\left(\frac{i}{\hbar}\int_0^{\tilde{T}}dtH_{\rm int}^{(0)}[\tilde{r}(t)]\right)\right.\right. \times\left.\left.\exp\left(-\frac{i}{\hbar}\int_0^{T}dtH_{\rm int}^{(0)}[r(t)]\right)\right|n_i\right\rangle \tag{93}$$

in the degenerate spectrum limit.

Since the exponents of the two operators in the influence functional commute, ρ_M becomes the matrix element of an SU(6) transformation between SU(6) basis states. In other words it is a representation matrix element for this group and can easily be calculated using standard techniques. The two-time influence functional for the sd version of the interacting boson model was calculated by Balantekin *et al.* (1992) and, for the particular case of SU(3) limit, by Balantekin *et al.* (1991).

B. Higher-order couplings

Up to this point, we have utilized only a first-order coupling between nuclear states and translational motion. Alternatively, one can include the effects of coupling to all orders. This can be achieved by exploiting the symmetry properties of the resolvent operator directly without utilizing its path-integral representation. Such a Green's-function approach has also been used to study quantum tunneling in a heat bath (Takigawa, Alhassid, and Balantekin, 1992).

To include the effects of couplings to all orders, the interaction Hamiltonian in Eq. (33) is written as

$$H_{\rm int}(\mathbf{r},\xi)+V_0(r)=V_{\rm Coul}(\mathbf{r},\xi)+V_{\rm nuc}(\mathbf{r},\xi), \tag{94}$$

where the Coulomb part is

$$V_{\rm Coul}(\mathbf{r},\xi)=\frac{Z_1Z_2e^2}{r}\left(1+\frac{3}{5}\frac{R_1^2}{r^2}\,\hat{O}\right)\quad(r>R_1),$$
$$=\frac{Z_1Z_2e^2}{r}\left(1+\frac{3}{5}\frac{r^2}{R_1^2}\,\hat{O}\right)\quad(r<R_1). \tag{95}$$

The nuclear part is taken to have Woods-Saxon form,

$$V_{\rm nuc}(\mathbf{r},\xi)=-V_0\left\{1+\exp\left[\frac{r-R_0-R_1\hat{O}(\hat{\mathbf{r}},\xi)}{a}\right]\right\}^{-1}. \tag{96}$$

In Eqs. (95) and (96), R_0 is the sum of the target and projectile radii and R_1 is the mean radius of the deformed target. $\hat{O}$ is a general coupling operator between the internal coordinates and the relative motion

$$\hat{O}=\sum_k v_k T^{(k)}(\xi)\cdot Y^{(k)}(\hat{\mathbf{r}}). \tag{97}$$

The coefficients v_k represent the strengths of the various multipole transitions in the target nucleus. In the standard IBM with s and d bosons, the only possible transition operators have $k=0,2,4,\ldots$ (odd values being excluded as a consequence of the reflection symmetry of the nuclear shape). The monopole contribution is already included in the Woods-Saxon parametrization and so is not needed. The quadrupole and hexadecapole operators are given by

$$T^{(2)}=[s^\dagger\tilde{d}+d^\dagger s]^{(2)}+\chi[d^\dagger\tilde{d}]^{(2)}, \tag{98}$$

$$T^{(4)}=[d^\dagger\tilde{d}]^{(4)}. \tag{99}$$

We adopt the "consistent-Q" formalism of Casten and Warner (1988), in which χ in Eq. (98) is taken to be the same as in $H_{\rm IBM}$ (fitted to reproduce the energy-level scheme and the electromagnetic transition rates of the target nucleus) and is thus not a free parameter.

In the previous section, we used the usual approximation in which the nuclear potential of Eq. (96) is expanded in powers of the coupling, keeping only the linear term [cf. Eq. (88)]. In order to calculate the fusion cross section to all orders, we consider the resolvent operator for the system

$$G^+(E)=\frac{1}{E^+-H_t-H_{\rm IBM}(\xi)-H_{\rm int}(r,\hat{O})}. \tag{100}$$

The basic idea is to identify the unitary transformation which diagonalizes the operator $\hat{O}$,

$$\hat{O}_d=\mathcal{U}\hat{O}\mathcal{U}^\dagger, \tag{101}$$

in order to calculate its eigenvalues and eigenfunctions,

$$\hat{O}_d|n\rangle=\zeta_n|n\rangle. \tag{102}$$

Assuming the completeness of these eigenfunctions,

$$\sum_n |n\rangle\langle n|=1, \tag{103}$$

one can write the matrix element of the resolvent as

$$\begin{aligned}
&\langle\xi_f,r_f|G^+(E)|\xi_i,r_i\rangle\\
&\quad=\langle\xi_f,r_f|\mathcal{U}^\dagger\mathcal{U}[E^+-H_t-H_{\rm int}(r,\hat{O})]^{-1}\mathcal{U}^\dagger\mathcal{U}|\xi_i,r_i\rangle\\
&\quad=\langle\xi_f,r_f|\mathcal{U}^\dagger[E^+-H_t-H_{\rm int}(r,\hat{O}_d)]^{-1}\\
&\qquad\times\sum_n |n\rangle\langle n|\mathcal{U}|\xi_i,r_i\rangle\\
&\quad=\sum_n \langle\xi_f|\mathcal{U}^\dagger|n\rangle\langle n|\mathcal{U}|\xi_i\rangle\langle r_f|G_n^+|r_i\rangle
\end{aligned} \tag{104}$$

where

$$G_n^+(E)=\frac{1}{E^+-H_t-H_{\rm int}(r,\zeta_n)}. \tag{105}$$

To derive this result we ignore the excitation energies in the target nucleus. This corresponds to setting the term $H_{\rm IBM}$ to zero in Eqs. (100) and (105). In this case, the $G_n^+(E)$ given in Eq. (104) is the resolvent operator for one-dimensional motion in the potential $H_{\rm int}(r,\zeta_n)$, the fusion cross section of which can easily be calculated within the standard WKB approximation. The total cross section can be calculated by multiplying these eigenchannel cross sections by the weight factors indicated in Eq. (104). The calculation of the matrix element $\langle n|\mathcal{U}|\xi_i\rangle$ within the IBM is straightforward (Balantekin *et al.*, 1993, 1994a, 1994b). It is also possible to generalize the previous formalism to include arbitrary kinds of bosons in the target nucleus and investigate whether g bosons have any discernible effects on subbarrier fusion reactions. One finds (Balantekin *et al.*, 1994b) that except for slight differences in the barrier distributions (which can be made even smaller by fine-tuning the coupling strengths), there are no visible differences between the sd and sdg model predictions. The similarity of the results implies that subbarrier fusion probes the overall coupling strength in nuclei, but otherwise is not sensitive to the details of the nuclear wave functions. In this sense subbarrier fusion, which is an inclusive process, is in the same category as other static quantities (energy levels, electromagnetic transition rates) and does not seem to constitute a dynamic probe of nuclei, in contrast to exclusive processes such as proton scattering.

Using this formalism, a systematic study of subbarrier fusion of ^{16}O with rare-earth nuclei became possible. Fusion cross sections for the reactions ^{16}O+^{144,148,154}Sm and ^{16}O+^{186}W were measured by the Australian National University group (Wei *et al.*, 1991; Leigh *et al.*, 1993, 1995; Lemmon *et al.*, 1993; Morton *et al.*, 1994). The angular momentum distributions for ^{16}O+^{154}Sm were measured by Bierman *et al.* (1993) and for ^{16}O+^{152}Sm by Wuosmaa *et al.* (1991). Those for ^{16}O+^{144,148}Sm were deduced by Baba (1993). Balantekin *et al.* (1994a) fit the existing data on vibrational and rotational nuclei with a consistent set of parameters, which they then used to predict the cross section and $\langle\ell\rangle$ distributions. Figure 8 compares those data with the cross-section calculations of Balantekin *et al.* (1994a) and the angular momentum distribution calculations of Balantekin *et al.* (1994c).

Finally one should mention that the effects of anharmonicities both in nuclear spectra (Casten and Zamfir, 1996) and in the vibrational coupling in subbarrier fusion (Hinde *et al.*, 1994; Morton, 1995) have recently attracted some attention. Arima and Iachello (1976) pointed out that the U(5) symmetry limit of the IBM should exhibit anharmonicities in the spectra similar to the geometric anharmonic vibrator model of Brink *et al.* (1965). This assertion was later explicitly confirmed (Aprahamian *et al.*, 1987). This feature of the interacting boson model makes it possible to discuss the effects of

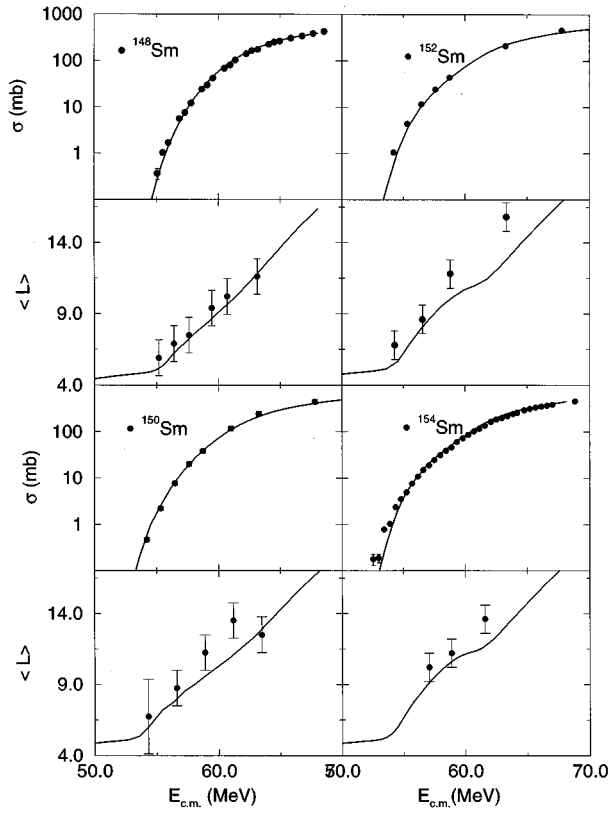

FIG. 8. A systematic study of subbarrier fusion of an ^{16}O projectile with rare earth nuclei, the structure of which is described using the interacting boson model (see text).

anharmonicities in the vibrational coupling in subbarrier fusion using the U(5) limit (Hagino, Takigawa, and Kuyucak, 1997).

V. COMPARISON OF CURRENT THEORY WITH DATA

A. Status of coupled-channels calculations

DiGregorio and Stokstad (1991) presented a systematic analysis of fusion cross sections and average angular momenta for fourteen different systems, using a barrier penetration model that includes coupling to inelastic channels. They concluded that model predictions explain data well for light and asymmetric systems, whereas large discrepancies exist for large symmetric systems. Indeed, for light and asymmetric systems the basic premise of the coupled-channels calculations is justified: For these systems the repulsive Coulomb potential is relatively weak and the tail of the attractive nuclear potential has sufficient strength to ''turn it around'' to form the potential barrier. The barrier is thus formed at a rather large nuclear separation, long before two nuclear surfaces start touching. Consequently, as the system penetrates the barrier, individual nuclei preserve their character and one can talk about coupling of the states in the target nuclei to the quantum tunneling process. The inversion procedure of Balantekin *et al.* (1983) demonstrated that even when there were isotopic differences in the fusion cross section (Wu *et al.*, 1985), one could still describe the quantum tunneling with a one-dimensional *effective* potential for very light systems. On the other hand, for heavier and more symmetric systems, other effects not explicitly included in the coupled-channels calculations, such as neck formation, may play an important role.

Many experimental groups use simplified coupled-channels codes such as CCFUS (Dasso and Landowne, 1987b), CCDEF (Fernandez-Niello *et al.*, 1989), CCMOD (Dasgupta *et al.*, 1992), or the IBM-based models (Balantekin *et al.*, 1993, 1994a, 1994b). As we mentioned earlier it is worthwhile to keep in mind that, although these codes are quite adequate for qualitative comparisons, they may be making a number of assumptions, such as ignoring the radial dependence of the coupling form factor, excitation energies, and/or higher-order couplings. Before one makes a quantitative statement, it may be sagacious to check what the approximations are and if the observed discrepancies with the data are a result of these simplifications. In Sec. IV.B we explicitly demonstrated the effects of higher-order couplings.

The crucial ingredient of the coupled-channels calculations is to identify relevant degrees of freedom and to model the appropriate Hamiltonian. Even the choice of the optical potential should be scrutinized. For example, a recent survey (Brandan and Satchler, 1997) of current knowledge of the optical potential between even much simpler systems, such as two light ions, indicates that many anomalies need to be resolved before a good theoretical understanding of the elastic scattering data can be achieved. For heavier systems, from fits to elastic scattering data at energies near the barrier, the optical potential was shown to have a strong energy dependence, known as a ''threshold anomaly'' (Satchler, 1991). Nagarajan *et al.* (1985) pointed out that the dispersion relation between the real and imaginary parts of the optical potential should be used in regions where the absorption varies rapidly with energy, such as near and below the barrier. The source of the energy dependence could be either channel coupling or the nonlocality of the exchange contribution (Galetti and Candido Ribeiro, 1994). Galetti and Candido Ribeiro (1995) compared nonlocal effects and coupled-channels calculations in simple models of nuclear fusion.

The very first coupled-channels calculations for heavy-ion fusion assumed a linear coupling to quadrupole or octupole surface vibrations and quadrupole deformations. As more precise data became available, the significance of the hexadecapole deformations (Rhodes-Brown and Oberacker, 1983), neutron transfer (Broglia, Dasso, Landowne, and Pollarolo, 1983), coupling of multiphonon states (Takigawa and Ikeda, 1986; Kruppa *et al.*, 1993), and higher-order couplings (Balantekin *et al.*, 1993) emerged. In the rest of this section we discuss representative data illustrating these effects.

B. Nucleon transfer

Another interesting question is the effect of nucleon transfer on subbarrier fusion (see Sec. III.B). In particu-

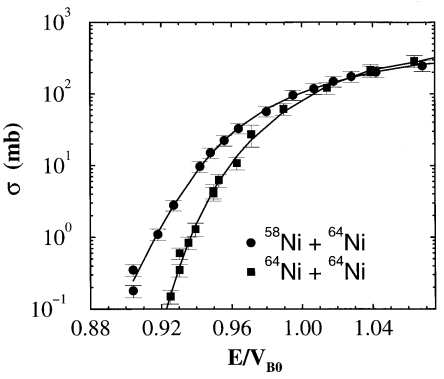

FIG. 9. Fusion cross sections from Ackermann *et al.* (1996) for the systems ^{58}Ni+^{64}Ni (circles) and ^{64}Ni+^{64}Ni (squares) as a function of the energy normalized to the barrier height.

lar the role of transfer channels with positive Q values has been emphasized (Broglia, Dasso, Landowne, and Pollarolo, 1983; Broglia, Dasso, Landowne, and Winther, 1983; Esbensen and Landowne, 1989). Algebraic models like that described in Sec. IV at present do not include the effects of nucleon transfer. It is now experimentally possible to observe up to six-nucleon transfer at subbarrier energies (Jiang *et al.*, 1994). Hence in the near future systematic studies including nucleon transfer reactions, fusion, and elastic scattering may be possible.

The effect of nucleon transfer on fusion can be illustrated, for example, by considering fusion reactions between different Ni isotopes. Indeed, these were the pioneering experiments of Beckerman *et al.* (1980), in which the enhancement of subbarrier fusion cross sections was first observed. These cross sections were later measured by Schicker *et al.* (1988) and more recently by Ackermann *et al.* (1996). The cross sections measured by Ackermann *et al.* (1996) for the ^{58}Ni+^{64}Ni and ^{64}Ni+^{64}Ni systems are displayed in Fig. 9, where the energies are normalized to the height of the s-wave potential barrier. One sees a discernible enhancement for the ^{58}Ni+^{64}Ni system over the ^{64}Ni+^{64}Ni system. In the symmetric system ^{64}Ni+^{64}Ni there are no transfer channels with positive Q values, and only those channels describing inelastic excitations need to be included. On the other hand, in the ^{58}Ni+^{64}Ni system there is an additional coupling of the transfer channel ^{64}Ni(^{58}Ni,^{60}Ni)^{62}Ni with a Q value of $Q=+3.9$ MeV. These additional channels increase the ^{58}Ni+^{64}Ni cross section (cf. the discussion in Sec. III.B).

Signatures of positive-Q-value transfer reactions can also be identified in fusion barrier distributions. By comparing barrier distributions for ^{16}O+^{144}Sm and ^{17}O+^{144}Sm reactions, Morton *et al.* (1994) showed that the effect of the neutron-stripping channel in the second reaction is evident in the barrier distribution.

In fusion reactions of identical nuclei there are a number of interesting effects magnified by the existence of only even partial waves. For example, the fusion cross sections have an oscillatory structure as a function of energy (Poffe *et al.*, 1983). Furthermore, elastic transfer plays an important role in such collisions (von Oertzen and Nöremberg, 1973). Christley *et al.* (1995) showed that, even in cases where no oscillatory structure is visible in cross section, there still is a signature of the elastic transfer in the barrier distributions.

C. Probing asymmetry effects

One way to probe the effects of asymmetry of the system other than nucleon transfer is to measure fusion cross sections and average angular momenta for different systems leading to the same compound nucleus. Such a measurement was recently performed (Ackermann *et al.*, 1996) for the systems ^{28}Si+^{100}Mo and ^{64}Ni+^{64}Ni leading to the compound nucleus ^{128}Ba. These measurements complement a previous measurement for the system ^{16}O+^{112}Cd (Ackerman *et al.*, 1994). They find that both fusion cross sections and average angular momenta can be explained by coupled-channels calculations. For the ^{28}Si+^{100}Mo system, including lowest 2^+ and 3^- states of both the target and the projectile in the coupled-channels calculation improves the agreement between theory and data, as compared to the no-coupling limit, but is not sufficient to reproduce the data. One needs to include an additional channel with the Q value of the two-neutron pickup reaction to bring the data and theory into agreement. The data for the symmetric system ^{64}Ni+^{64}Ni, where no transfer channels with positive Q values are present, are already well reproduced with coupling only to the inelastic channels. Hence the data of Ackermann *et al.* (1996) also provide evidence for the influence of two-nucleon transfer channels with positive Q values on fusion probabilities.

Studies of transfer channel coupling and entrance channel effects for the near and subbarrier fusion were also carried out by Prasad *et al.* (1996) for the systems ^{46}Ti+^{64}Ni, ^{50}Ti+^{60}Ni, ^{19}F+^{93}Nb and by Charlop *et al.* (1995) for the systems ^{28}Si+^{142}Ce, ^{32}S+^{138}Ba, and ^{48}Ti+^{122}Sn. These authors report no significant entrance channel effects except that the positive Q value for two-neutron pickup shows up as an additional enhancement in the ^{46}Ti+^{64}Ni system.

D. Signatures of nuclear vibrations

One relatively unexplored aspect of subbarrier fusion is the presence of signatures of nuclear vibrations. Leigh *et al.* (1995) confirmed the effects of vibrational coupling in the ^{16}O+^{144}Sm system. To search for signatures of nuclear vibrations Stefanini *et al.* (1995b) measured the fusion cross section for ^{32,36}S+^{110}Pd systems. ^{110}Pd is a vibrational nucleus whose two-quadrupole-phonon triplet is well known. Simplified coupled-channels calculations for these systems have been performed by Stefanini *et al.* (1995b) and by DeWeerd (1996). Stefanini *et al.* (1995b), using the method of Kruppa *et al.* (1993), assumed a constant coupling explicitly including the finite Q value of the coupled channels. In these experiments it was also observed that the cross section for the ^{32}S+^{110}Pd system is greatly enhanced because of the two-neutron transfer channel.

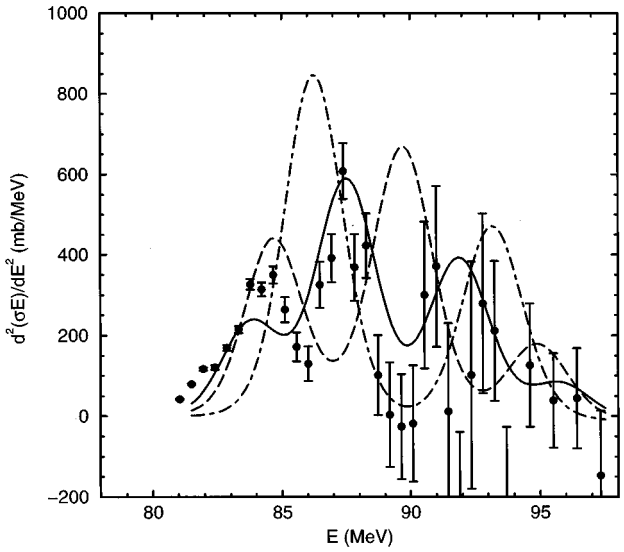

FIG. 10. Comparison between measured and calculated barrier distributions for a ^{36}S+^{110}Pd system as more phonons are included in the calculation. The data are from Stefanini *et al.* (1995c) and the calculation is from DeWeerd (1996). The dot-dashed, dashed, and solid lines correspond to calculations including one-phonon, two-phonon, and three-phonon states, respectively.

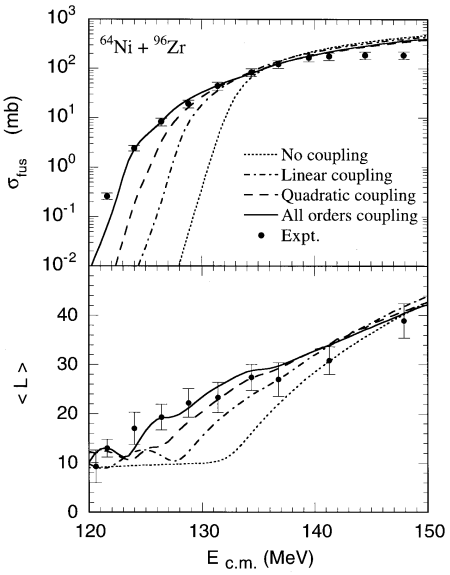

FIG. 11. Fusion cross section (upper panel) and the average angular momenta (lower panel) for the ^{64}Ni+^{96}Zr system. The data are from Stefanini *et al.* (1992), and the theoretical calculation is from Hagino, Takigawa, Dasgupta *et al.* (1997). The two-phonon states of the quadrupole surface vibration of both the projectile and the target are taken into account in the coupled-channels calculations. The dotted line is the result in the absence of channel coupling. The dot-dashed and dashed lines are the results when the nuclear potential is expanded up to the first- and the second-order terms in the deformation parameters, respectively. The solid line is the result of the coupled-channels calculations to all orders, obtained without expanding the nuclear potential.

Since ^{110}Pd lies between U(5) and SO(6) symmetry limits of the interacting boson model, it cannot be described analytically. DeWeerd (1996) first numerically calculated quadrupole matrix elements between different states using the PHINT code (Scholten, 1991) and then numerically obtained eigenvalues and the associated weights [cf. Eq. (104)]. His result for the barrier distribution of the ^{36}S+^{110}Pd system is displayed in Fig. 10 along with the data. While one-phonon space clearly fails in describing the barrier distribution, the agreement with data successively improves as one includes more phonons in the calculation. This drastic change in the barrier distribution for different numbers of phonons was also noted by Stefanini *et al.* (1995b) for this system and by Stefanini *et al.* (1995c) for the ^{58}Ni+^{60}Ni system.

E. Effects of nonlinear couplings

The effects of nonlinear couplings are an important component in the theoretical description of subbarrier fusion data. These effects were discussed by Balantekin *et al.* (1993) using the IBM in the limit of zero excitation energy (cf. Sec. IV.B). For nuclear surface vibrations the excitation energies cannot be neglected in most cases, and one has to solve full coupled-channels equations. These calculations can be very involved, and consequently they have been carried out by very few groups.

Esbensen and Landowne (1987) expanded the coupling potential [see Eq. (96)] up to second order with respect to the deformation parameter, obtaining a good agreement between their calculations and data for fusion cross sections between different nickel isotopes. The quadratic coupling approximation was shown to describe fusion cross sections and angular momentum distributions well for the ^{58,64}Ni+^{92,100}Mo reactions (Rehm *et al.*, 1993). Coupled-channels calculations including coupling to all orders and the finite excitation energy of nuclear surface vibrations were performed for the ^{58}Ni+^{60}Ni reaction (Stefanini *et al.*, 1995c).

In Fig. 11 the calculation of Hagino *et al.* (1997) for the system ^{64}Ni+^{96}Zr is compared with the data of Stefanini *et al.* (1992). Here the results of coupled-channels calculations to all orders (solid lines) agree with the data very well, as opposed to the no-coupling (dotted lines), linear coupling (dot-dashed lines), and quadratic coupling (dashed lines) cases. The upper panel compares theory and calculations for the fusion cross section, while the lower panel does so for the average angular momenta. In this calculation up to double-phonon states are included in the coupled channels. An important feature of this calculation is that a truncation of the coupling within the double-phonon space, even at the quadratic level, is not sufficient to describe the data; one needs to include couplings to all orders.

F. Angular momentum distributions

DiGregorio and Stokstad (1991) also compared average angular momenta obtained using different experi-

mental techniques with theoretical predictions. They found that there is good agreement between theory and data obtained from isomer ratio and gamma-ray multiplicity measurements, with the exception of more symmetric systems, but not for the fission-fragment measurements. From the fission-fragment angular anisotropy measurements one obtains not $\langle \ell \rangle$, but $\langle \ell^2 \rangle$. Especially if the σ_ℓ distribution is pushed to higher ℓ values as a result of coupling to other channels, $\langle \ell^2 \rangle^{1/2}$ may significantly differ from $\langle \ell \rangle$, which may explain some of the reported discrepancies. An excellent review of efforts to measure angular momentum distributions in fusion reactions is that of Vandenbosch (1992).

There have been many attempts to extract average angular momenta directly from the fusion excitation functions (Reisdorf *et al.*, 1985; Balantekin and Reimer, 1986; Rowley *et al.*, 1993; Balantekin *et al.*, 1996). Moments of angular momenta are related to the moments of fusion cross sections (Balantekin *et al.*, 1996). These relations can help assess the consistency of accurate fusion cross-section measurements with measurements extracting angular momentum distributions using different methods.

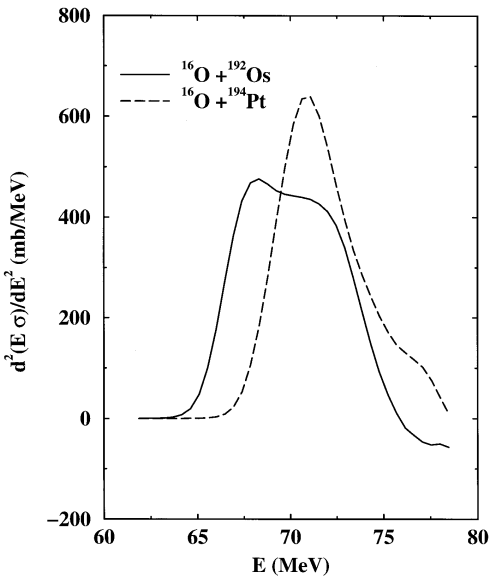

FIG. 12. Predicted behavior of the barrier distributions for fusion reactions on the prolate (^{194}Os) and the oblate (^{194}Pt) nuclei (Balantekin *et al.*, 1994a).

G. Probing shape-phase transitions with fusion

Until recently little attention was paid to subbarrier fusion on gamma-unstable targets. The Os and Pt region is interesting to study since these nuclei go through a shape transition from prolate to oblate as one increases the number of protons from 76 to 78. ^{192}Os has a positive (prolate) quadrupole deformation parameter and a negative hexadecapole deformation parameter. ^{194}Pt has a quadrupole deformation parameter similar in magnitude to those of ^{192}Os, but with a negative sign (oblate) and a hexadecapole deformation parameter comparable to that of ^{192}Os in sign and magnitude. The isotopes are similar in all respects other than the β_2 sign. The effect of this shape phase transition on the barrier distributions would be noticeable by the skewness toward higher energies for prolate nuclei and toward lower energies for oblate nuclei (Balantekin *et al.*, 1994a). Barrier distributions calculated by Balantekin *et al.* (1994a) using a model based on the IBM of Sec. IV, are shown in Fig. 12.

In an effort to understand this effect of the shape phase transition on the barrier distributions, the fusion cross sections for transitional nuclei Pt and Os were recently measured using an ^{16}O beam by the Legnaro group (Stefanini *et al.*, 1995a) and a ^{40}Ca beam by the Seattle group (Bierman *et al.*, 1996a). (Since ^{40}Ca is a heavier projectile, one expects this effect to be enhanced). The total fusion cross sections calculated by Balantekin *et al.* (1994a) for the ^{16}O+^{194}Pt system agree very well with the evaporation residues measured by Stefanini *et al.* (1995a) once the fission cross sections estimated by the statistical model are subtracted.

The ^{40}Ca+^{194}Pt and ^{40}Ca+^{192}Os cross sections measured and the associated barrier distributions extracted by Bierman *et al.* (1996a) are shown in Fig. 13, where the results are also compared with the CCDEF calculations. The calculations take the excitations of the target nucleus into account within a rotational model including both quadrupole and hexadecapole deformations. They also take into account the excitation of the projectile to the 3^- state at 3.7 MeV and the two-neutron transfer reactions from the target nucleus to the ground state of

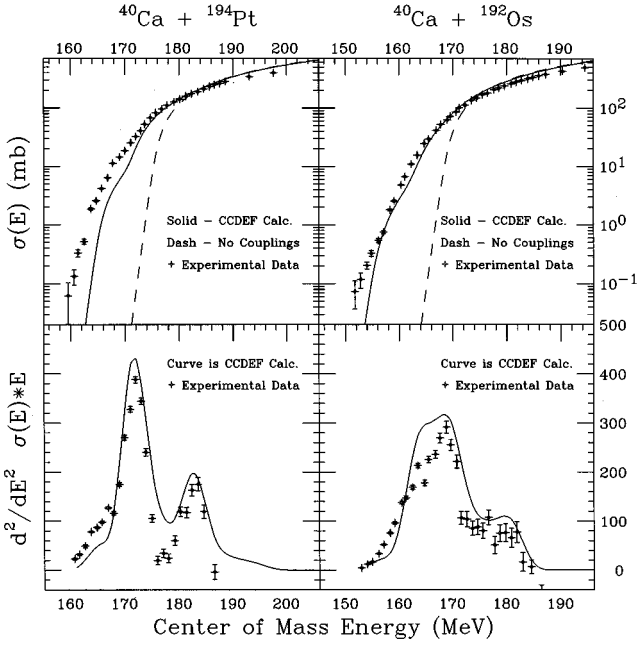

FIG. 13. Experimentally determined fusion cross sections by Bierman *et al.* (1996a) for prolate and oblate nuclei. The solid curve is the simplified coupled-channels calculation with the CCDEF code. The dashed curve is the result for a one-dimensional barrier ignoring all the couplings.

^{42}Ca. The constant-coupling approximations have been used for vibrational excitation of the projectile and the transfer reactions, while the radial dependence of the form factor of the collective model was used for rotational excitations. The predicted skewness of the barrier distribution toward higher energies for the prolate nucleus ^{194}Os and toward lower energies for the oblate nucleus ^{194}Pt is observed. The second peak for both systems is due to the excitation of the octupole state in the projectile. The barrier distributions for both systems also exhibit a tail at the lower energies, which is not reproduced by the CCDEF calculations. This problem was recently associated with the contribution of the two-nucleon transfer reactions to the first excited 2^+ state of ^{42}Ca (Bierman *et al.*, 1996b).

One should point out that the fusion barrier distribution extracted from the ^{16}O+^{186}W data of Lemmon *et al.* (1993) has the shape expected for a target nucleus with a negative hexadecapole deformation. There are pronounced differences between this distribution and that of ^{16}O+^{154}Sm (Wei *et al.*, 1991), which are just those expected from a change in sign of the hexadecapole deformation. These data thus demonstrate the strong sensitivity of fusion to the hexadecapole deformation.

H. Difficulties in extracting barrier distributions

Since barrier distributions include the second energy derivative of the cross section, very accurate measurements of excitation functions at closely spaced energies are required. Even with very-high-precision data, smooth barrier distributions can only be obtained under certain model-dependent assumptions such as fine-tuning the energy spacing for calculating second derivatives (Izumoto *et al.*, 1995; DeWeerd, 1996). Krappe and Rossner (1995) suggested using integrals, rather than the derivatives of the fusion data, to improve model independence in the analyses. Unfortunately, moments of the cross sections are even more featureless than the cross sections themselves (Balantekin *et al.*, 1996). In contrast, one of the main advantages of using barrier distributions is that they bring out important features in the data. However, moments of the cross section could be useful as they are related to the moments of angular momenta under certain assumptions (Balantekin and Reimer, 1986; Dasso *et al.*, 1986; Esbensen and Landowne, 1987; Balantekin *et al.*, 1996).

Even with a very high precision in the fusion cross section it is rather difficult to extract fusion barrier distributions at higher energies, as the cross section changes very slowly and the errors on the barrier distribution grow with energy. To illustrate the reason for this behavior, consider a set of fusion data measured at a fixed energy spacing ΔE. The second derivative may be approximated by the point-difference formula (Rowley, 1992)

$$\left[\frac{d^2(E\sigma)}{dE^2}\right]_n = -\frac{2(E\sigma)_n-(E\sigma)_{n+1}-(E\sigma)_{n-1}}{(\Delta E)^2}. \quad (106)$$

If the statistical errors on the cross section are a fixed fraction of their measured values,

$$(\delta\sigma)_n = f\sigma_n, \quad (107)$$

then the error in the second derivative is

$$\delta\left[\frac{d^2(E\sigma)}{dE^2}\right] \sim \frac{\sqrt{6}fE\sigma}{(\Delta E)^2}. \quad (108)$$

Hence the error in the second derivative increases as the cross section increases, whereas the second derivative itself gets smaller at higher energies. Furthermore ΔE must be small enough to resolve any interesting structure, which also contributes to the large errors at high energies.

It has been suggested that information about the barrier distributions may be contained in the quasielastic scattering excitation functions at backward angles (Kruppa *et al.*, 1993; Andres *et al.*, 1988). Timmers *et al.* (1995) recently developed a method of extracting a representation of the fusion barrier distribution from quasielastic excitation functions. They found that, although this representation of the quasielastic scattering data indeed shows the general features of the fusion barrier distributions, its sensitivity is reduced at high energies. More recently Rowley *et al.* (1996) showed that the effects of strong coupling are present in the barrier distributions from the elastic scattering, but are smoothed out since different eigenbarriers have phase differences. Furthermore the effects are also smoothed by weak couplings, which appear in first order in the elastic-scattering cross section, but only in second order in the fusion cross section. It would be important to treat the phase problem properly in order to obtain information on barrier distributions from the elastic-scattering data.

I. Fusion of unstable nuclei

Heavy-ion fusion reactions induced by a halo nucleus or by an unstable neutron-rich nucleus are very intriguing current subjects of nuclear physics (Ishihara *et al.*, 1993). Several groups have performed experiments to examine whether the fusion cross section in such cases is significantly different from that in heavy-ion collisions induced by the corresponding stable isotopes. Yoshida *et al.* (1995) studied the fusion reactions of ^{11,10,9}Be with ^{209}Bi at energies near the Coulomb barrier. They observed no significant difference in the excitation function for the collision of ^{11}Be from that of ^{10}Be. On the other hand, Fukou-Youmbi *et al.* (1994) have reported that the induced fission cross section near the Coulomb barrier is much larger in the ^{11}Be+^{238}U reaction than that in the ^{9}Be+^{238}U reaction. This is a very interesting result, though it is not clear yet whether the fission took place via a compound-nucleus formation, suggesting an enhanced fusion cross section in the case of unstable isotope.

Takigawa and Sagawa (1991) and Takigawa, Sagawa, and Shinozuka (1992) suggested that the fusion cross section will be significantly enhanced if one uses a halo

nucleus as the projectile. In deriving this conclusion, they assumed the existence of a stable soft dipole oscillation of the core nucleons against the halo neutrons. Though it is not yet completely settled, the existence of a physical soft dipole oscillation in light halo nuclei is unlikely (Sagawa *et al.*, 1995). This might explain why the fusion data of Yoshida *et al.* (1995) do not show any characteristically different behavior for the case of a ^{11}Be projectile. As has been shown by Takigawa and Sagawa (1991), the neutron halo itself can enhance the fusion cross section by statically lowering the fusion barrier. This effect alone however, is not so drastic. Moreover, ^{11}Be has a less pronounced halo property than ^{11}Li.

Using time-dependent Hartree-Fock theory, Kim *et al.* (1994) showed that nucleon transfer is enhanced for fusion reactions between a stable and an unstable nucleus with neutron halo.

There is some debate concerning the effects of breakup of the halo nuclei. Takigawa *et al.* (1993) have shown that, although the large enhancement of the fusion cross section is moderated by the breakup, the halo nucleus ^{11}Li still leads to a larger fusion cross section than the other Li isotopes. One should point out that this conclusion relies on the assumption that there exists a soft dipole resonance in ^{11}Li. On the other hand, Canto *et al.* (1995) argued that the fusion cross section of a halo nucleus would be hindered by the breakup effect, whereas Dasso and Vitturi (1994) contended that the breakup channel would enhance the fusion probability. In order to reach a definite conclusion, one needs to know more about the radial dependence of the breakup form factor and one needs to treat both the real and the virtual breakup processes in a consistent way, including the associated potential renormalization.

One interesting subject to be explored is the effects of bond formation due to halo neutrons on the fusion cross section. Bertulani and Balantekin (1993) studied this problem by using the fusion between ^{11}Li (consisting of ^{9}Li core and halo dineutrons) and ^{9}Li as an example. As ^{11}Li and ^{9}Li approach each other, there is a particular separation distance at which both the Coulomb and nuclear potentials between the two cores are small, but the two neutrons in the halo can be shared by both cores. One can then investigate the effect of this molecular bonding on the fusion of ^{11}Li and ^{9}Li. These preliminary calculations (Bertulani and Balantekin, 1993) indicated a very significant enhancement of the fusion cross section due to molecular bonding. Takigawa, Yoshida, Hagino, and Patra (1995) showed that this cross section is somewhat reduced when different initial conditions are used. The calculations of both groups were done in the adiabatic approximation, which tends to overestimate the effect. The existence of molecular bonding and its effect on the fusion process remain open questions.

In this connection, we wish to remark that a polarization of the wave functions of the valence neutrons, i.e., the admixture of higher orbits, is essential in order for the bond effect to be significant. Imanishi and von Oertzen (1995) studied the bond effect in the fusion between ^{11}Be and ^{10}Be and showed that a significant polarization of the valence nucleons starts to take place even where the core nuclei are still far apart if the binding energy of the valence nucleons is small, and that consequently there exists a large bond effect in this system. One notes that ^{11}Be has two bound states, $1p^{-}_{1/2}$ and $2s^{+}_{1/2}$, and one low-lying resonance state $1d^{+}_{5/2}$. The hybridization of these opposite-parity configurations causes a large polarization.

It is possible that the response of the projectile in heavy-ion collisions induced by a neutron-rich unstable nucleus can be formulated in terms of the coupling to a resonance state. Several models exist for calculating the effect of the width of the resonant state on quantum tunneling (Balantekin and Takigawa, 1985; Hussein *et al.*, 1995).

J. Fusion of very massive systems and superheavy nuclei

As the compound nuclei formed by fusion get heavier, fission becomes an increasingly important deexcitation channel. For such reactions, evaporation residues and fission fragments must be added to obtain the total fusion cross section. As systems get more massive ($Z_pZ_t > 1000$), fusion starts competing with other reaction channels representing a significant exchange of energy, charge, mass, and angular momenta. Understanding the dynamics of fusion and competing reactions for very massive systems is essential, among other things, to assess the conditions for the formation of superheavy elements. These topics are covered in a recent review by Reisdorf (1994).

A significant difference between the fusion of massive nuclei and the fusion of the medium-weight nuclei we have been discussing up until now is that the fusion cross section for very massive systems is not enhanced, but rather hindered. This situation is encountered when the product of the atomic numbers of the projectile and target exceeds about 1800 (Reisdorf, 1994). The incident energy has to be considerably higher than the fusion barrier expected from the Bass potential (Bass, 1974), which was determined to fit the fusion data above the barrier for medium-weight systems with $Z_pZ_t = 64-850$ in a potential model. This excess energy is called the extra push energy. Bjornholm and Swiatecki (1982) attributed it to the fact that the fission barrier for massive systems is located well inside the potential barrier in the entrance channel, and introduced the concepts of the extra push and the extra extra push. The former is the energy needed to overcome the conditional saddle, i.e., the saddle under the constraint of mass asymmetry, while the latter is the energy needed to carry the system inside the unconditional saddle for fission. Though there have been quite a number of experimental and theoretical studies of the extra push energy, its origin and dependence on various parameters of the system, such as the effective fissility parameter in the entrance channel, are not fully understood. One should note that the decrease of the fusion cross section with decreasing bom-

barding energy in massive systems, where there exists an extra push, is also much slower than that expected in the potential model where there exists an extra push. This indicates the existence of a kind of enhancement mechanism of the fusion cross section in massive systems, as well, once the hindrance effect associated with the extra push problem is isolated.

An interesting problem concerning the fusion of massive nuclei is the synthesis of superheavy elements. A significant advance occurred when Hofmann *et al.* (1996) at GSI, working with the SHIP velocity filter, succeeded in producing the superheavy element Z=112 by the so-called cold fusion method using the ^{70}Zn+^{208}Pb reaction. This is the heaviest element recorded to date and it is only two atomic numbers away from the predicted magic number Z=114. Though the successful synthesis of element 112 after the synthesis of elements 110 and 111 in 1994 seems to indicate that a similar experimental strategy can be used to go further into the realm of the heaviest elements, a problem is that the cross section is very small, i.e., of the order of 1 pb. Actually, only two events were identified for $Z=112$. It would certainly be very interesting to look for alternative ways to synthesize superheavy elements. An interesting question in this connection is whether there are advantages to using neutron-rich unstable nuclei. A preliminary study in this direction has been undertaken by Takigawa, Sagawa, and Shinozuka (1992) and Takigawa and Shinozuka (1992). These authors discussed the advantages, such as the larger survival probability of the compound system, lowering of the fusion barrier, and the possible lowering of the extra push energies, and disadvantages, such as the low beam intensity in reactions induced by neutron-rich unstable nuclei. In passing, we wish to mention that Nomura *et al.* (1995) are trying to use (HI, αxn) reactions to synthesize superheavy elements experimentally, using the cooling mechanism by α particle emission, and that Arimoto *et al.* (1997) are introducing a diffusion model to discuss theoretically the mechanism of the synthesis of superheavy elements, though both of them treat a thermal process rather than a quantum tunneling process.

VI. OPEN PROBLEMS AND OUTLOOK

Although there still are many unsettled issues even in fusion reactions with stable nuclei, remarkable progress has been made in the last fifteen years. New, conceptually alluring ways of analyzing data (such as studying barrier distributions), new approaches to channel coupling (such as the path-integral and Green's-function formalisms), and alternative methods of describing nuclear structure effects (such as those using the interacting boson model), have been introduced. The roles of nucleon transfer, higher-order couplings, and shape phase transitions have been elucidated. We can now understand the data for clean (i.e., asymmetric) systems in terms of inelastic excitations and nucleon transfer. Acquisition of high precision, complementary data for fusion, transfer reactions, and elastic scattering below and near the barrier should be encouraged as theoretical tools become available to analyze them.

On the other hand, fusion cross sections for very heavy symmetric systems cannot be reproduced by the present models. In such systems inclusion of higher-order coupling is essential. One salient ingredient is a proper description of neck formation. Though there are many pioneering attempts that relate the large enhancement of the fusion cross section to the neck formation (Jahnke *et al.*, 1982; Krappe *et al.*, 1983; Iwamoto and Harada, 1987; Iwamoto and Takigawa, 1989; Aguiar *et al.*, 1988), the microscopic description of fusion reactions in general and neck formation in particular is still at a very primitive stage and needs to be further developed. In connection with the former, we wish to note the computer simulations for subbarrier fusion reactions by Bonasera and Kondratyev (1994). The effects of neck formation could be formulated in terms of quantum tunneling in a multidimensional space (Kodama *et al.*, 1978; Landowne and Nix, 1981; Denisov and Royer, 1994, 1995).

Beams of short-lived radioactive nuclei at existing and at several now under construction experimental facilities present new opportunities to explore the dynamics of fusion reactions below the Coulomb barrier. In such facilities, in addition to testing our present understanding of the fusion dynamics in a new setting, we can investigate entirely new facets such as the coupling of resonant states to quantum tunneling and the possibility of molecular bond formation.

One should finally remark that there are many other tunneling phenomena in nuclear physics besides heavy-ion fusion reactions. Alpha decay, fission, various rare decays, and nuclear structure problems such as the decay of a superdeformed band to a normal band will also be affected by coupling to the intrinsic degrees of freedom, and insight obtained in the study of heavy-ion fusion reactions at subbarrier energies will be a valuable tool for understanding these phenomena in more detail.

ACKNOWLEDGMENTS

We thank J. Beacom and K. Hagino for their comments on the manuscript. We are grateful to our collaborators and colleagues J. Bennett, A. DeWeerd, K. Hagino, S. Kuyucak, J. Leigh, N. Rowley, and R. Vandenbosch for many discussions over the years. This research was supported in part by the U.S. National Science Foundation Grants No. PHY-9314131 and PHY-9605140; in part by the Japan Society of Promotion of Science; and in part by the University of Wisconsin Research Committee with funds granted by the Wisconsin Alumni Research Foundation. It was also supported in part by the Grant-in-Aid for General Scientific Research, Contracts No. 06640368 and No. 08640380; the Grant-in-Aid for Scientific Research on Priority Areas, Contracts No. 05243102 and No. 08240204; and Monbusho International Scientific Research Program: Joint Research from the Japanese Ministry of Education, Science and Culture Contract No. 09044051.

REFERENCES

Abe, M., and N. Takigawa, 1988, Phys. Lett. B **209**, 149.

Ackermann, D., 1995, Acta Phys. Pol. B **26**, 517.

Ackermann, D., P. Bednarczyk, L. Corradi, D. R. Napoli, C. M. Petrache, P. Spolaore, A. M. Stefanini, K. M. Varier, H. Zhang, F. Scarlassara, S. Beghini, G. Montagnoli, L. Müller, G. F. Segato, F. Soramle, and C. Signorini, 1996, Nucl. Phys. A **609**, 91.

Ackermann, D., L. Corradi, D. R. Napoli, C. M. Petrache, P. Spolaore, A. M. Stefanini, F. Scarlassara, S. Beghini, G. Montagnoli, G. F. Segato, and C. Signorini, 1994, Nucl. Phys. A **575**, 374.

Aguiar, C. E., V. C. Barbosa, L. F. Canto, and R. Donangelo, 1988, Phys. Lett. B **201**, 22.

Andres, M. V., N. Rowley, and M. A. Nagarajan, 1988, Phys. Lett. B **202**, 292.

Aprahamian, A., D. S. Brenner, R. F. Casten, R. L. Gill, and A. Piotrowski, 1987, Phys. Rev. Lett. **59**, 535.

Arima, A., and F. Iachello, 1976, Ann. Phys. (N.Y.) **99**, 253.

Aritomo, Y., T. Wada, M. Ohta, and Y. Abe, 1997, Phys. Rev. C **55**, R1011.

Baba, C. V. K., 1993, Nucl. Phys. A **553**, 719c.

Back, B. B., R. R. Betts, J. E. Gindler, B. D. Wilkins, S. Saini, M. B. Tsang, C. K. Gelbke, W. G. Lynch, M. A. McMahan, and P. A. Baisen, 1985, Phys. Rev. C **32**, 195.

Balantekin, A. B., J. R. Bennett, A. J. DeWeerd, and S. Kuyucak, 1992, Phys. Rev. C **46**, 2019.

Balantekin, A. B., J. R. Bennett, and S. Kuyucak, 1993, Phys. Rev. C **48**, 1269.

Balantekin, A. B., J. R. Bennett, and S. Kuyucak, 1994a, Phys. Rev. C **49**, 1079.

Balantekin, A. B., J. R. Bennett, and S. Kuyucak, 1994b, Phys. Rev. C **49**, 1294.

Balantekin, A. B., J. R. Bennett, and S. Kuyucak, 1994c, Phys. Lett. B **335**, 295.

Balantekin, A. B., J. Bennett, and N. Takigawa, 1991, Phys. Rev. C **44**, 145.

Balantekin, A. B., A. J. DeWeerd, and S. Kuyucak, 1996, Phys. Rev. C **54**, 1853.

Balantekin, A. B., S. E. Koonin, and J. W. Negele, 1983, Phys. Rev. C **28**, 1565.

Balantekin, A. B., and P. E. Reimer, 1986, Phys. Rev. C **33**, 379.

Balantekin, A. B., and N. Takigawa, 1985, Ann. Phys. (N.Y.) **160**, 441.

Bass, R., 1974, Nucl. Phys. A **231**, 45.

Beckerman, M., 1988, Rep. Prog. Phys. **51**, 1047.

Beckerman, M., M. Salomaa, H. A. Enge, A. Sperduto, J. Ball, A. DiRienzo, S. Gazes, Y. Chen, J. D. Molitoris, and M. Naifeng, 1980, Phys. Rev. Lett. **45**, 1472.

Bertulani, C., and A. B. Balantekin, 1993, Phys. Lett. B **314**, 275.

Bierman, J. D., P. Chan, J. F. Liang, M. P. Kelly, A. A. Sonzogni, and R. Vandenbosch, 1996a, Phys. Rev. Lett. **76**, 1587.

Bierman, J. D., P. Chan, J. F. Liang, M. P. Kelly, A. A. Sonzogni, and R. Vandenbosch, 1996b, University of Washington preprint.

Bierman, J. D., A. W. Charlop, D. J. Prindle, R. Vandenbosch, and D. Ye, 1993, Phys. Rev. C **48**, 319.

Bjornholm, S., and W. J. Swiatecki, 1982, Nucl. Phys. A **391**, 471.

Bonasera, A., and V. Kondratyev, 1994, Phys. Lett. B **339**, 207.

Brandan, M. E., and G. R. Satchler, 1997, Phys. Rep. **285**, 143.

Brink, D. M., 1985a, *Semi-Classical Methods for Nucleus-Nucleus Scattering* (Cambridge University, Cambridge, England).

Brink, D. M., 1985b, in *Frontiers of Nuclear Dynamics*, edited by R. A. Broglia and C. H. Dasso (Plenum, London), p. 171.

Brink, D. M., A. F. R. de Toledo Piza, and A. K. Kerman, 1965, Phys. Lett. **19**, 413.

Brink, D. M., M. C. Nemes, and D. Vautherin, 1983, Ann. Phys. (N.Y.) **147**, 171.

Brink, D. M., and U. Smilansky, 1983, Nucl. Phys. A **405**, 301.

Broglia, R. A., C. H. Dasso, S. Landowne, and G. Pollarolo, 1983, Phys. Lett. B **133**, 34.

Broglia, R. A., C. H. Dasso, S. Landowne, and A. Winther, 1983, Phys. Rev. C **27**, 2433.

Caldeira, A. O., and A. J. Leggett, 1983, Ann. Phys. (N.Y.) **149**, 374.

Canto, L. F., R. Donangelo, P. Lotti, and M. S. Hussein, 1995, Phys. Rev. C **52**, R2848.

Casten, R. F., and D. D. Warner, 1988, Rev. Mod. Phys. **60**, 389.

Casten, R. F., and N. V. Zamfir, 1996, Phys. Rep. **264**, 81.

Charlop, A., J. Bierman, Z. Drebi, A. Garcia, S. Gil, D. Prindle, A. Sonzogni, R. Vandenbosch, and D. Ye, 1995, Phys. Rev. C **51**, 628.

Chase, D. M., L. Wilets, and A. R. Edmonds, 1958, Phys. Rev. **110**, 1080.

Christley, J. A., M. A. Nagarajan, and A. Vitturi, 1995, Nucl. Phys. A **591**, 341.

Cole, M. W., and R. H. Good, 1978, Phys. Rev. A **18**, 1085.

Dasgupta, M., A. Navin, Y. K. Agarwal, C. V. K. Baba, H. C. Jain, M. L. Jhingan, and A. Roy, 1991, Phys. Rev. Lett. **66**, 1414.

Dasgupta, M., A. Navin, Y. K. Agarwal, C. V. K. Baba, H. C. Jain, M. L. Jhingan, and A. Roy, 1992, Nucl. Phys. A **539**, 351.

Dasso, C. H., H. Esbensen, and S. Landowne, 1986, Phys. Rev. Lett. **57**, 1498.

Dasso, C. H., and S. Landowne, 1987a, Phys. Lett. B **183**, 141.

Dasso, C. H., and S. Landowne, 1987b, Comput. Phys. Commun. **46**, 187.

Dasso, C. H., , S. Landowne, and A. Winther, 1983a, Nucl. Phys. A **405**, 381.

Dasso, C. H., S. Landowne, and A. Winther, 1983b, Nucl. Phys. A **407**, 221.

Dasso, C. H., and A. Vitturi, 1994, Phys. Rev. C **50**, R12.

Denisov, V. Y., and G. Royer, 1994, J. Phys. G **20**, L43.

Denisov, V. Y., and G. Royer, 1995, Phys. At. Nucl. **58**, 397.

DeWeerd, A. J., 1996, Ph.D. Dissertation, University of Wisconsin-Madison.

DiGregorio, D. E., J. O. Fernandez-Niello, A. J. Pacheco, D. Abriola, S. Gil, A. O. Macchiavelli, J. E. Testoni, P. R. Pascholati, V. R. Vanin, R. Liguori Neto, N. Carlin Filho, M. M. Coimbra, P. R. Silveira Gomes, and R. G. Stokstad, 1986, Phys. Lett. B **176**, 322.

DiGregorio, D. E., K. T. Lesko, B. A. Harmon, E. B. Norman, J. Pouliot, B. Sur, Y. D. Chan, and R. G. Stokstad, 1990, Phys. Rev. C **42**, 2108.

DiGregorio, D. E., and R. G. Stokstad, 1991, Phys. Rev. C **43**, 265.

Esbensen, H., 1981, Nucl. Phys. A **352**, 147.

Esbensen, H., and S. Landowne, 1987, Phys. Rev. C **35**, 2090.

Esbensen, H., and S. Landowne, 1989, Nucl. Phys. A **492**, 473.

Esbensen, H., and S. Landowne, 1989, Nucl. Phys. A **467**, 136.
Esbensen, H., S. Landowne, and C. Price, 1987, Phys. Rev. C **36**, 1216.
Esbensen, H., J.-Q. Wu, and G. F. Bertsch, 1983, Nucl. Phys. A **411**, 275.
Fernandez-Niello, J. O., C. H. Dasso, and S. Landowne, 1989, Comput. Phys. Commun. **54**, 409.
Fischer, R. D., A. Ruckelshausen, G. Koch, W. Kühn, V. Metag, R. Mühlhans, R. Novotny, H. Ströher, H. Gröger, D. Habs, H. W. Heyng, R. Repnow, D. Schwalm, W. Reisdorf, and R. S. Simon, 1986, Phys. Lett. B **171**, 33.
Fukou-Youmbi, V., J. L. Sida, and N. Alamanos, 1994, in *Heavy Ion Fusion, Exploring the Variety of Nuclear Properties*, edited by A. M. Stefanini *et al.* (World Scientific, Singapore), p. 305.
Galetti, D., and M. A. Candido Ribeiro, 1994, Phys. Rev. C **50**, 2136.
Galetti, D., and M. A. Candido Ribeiro, 1995, Phys. Rev. C **51**, 1408.
Ginocchio, J. N., T. Otsuka, R. D. Amado, and D. A. Sparrow, 1986, Phys. Rev. C **33**, 247.
Gomez-Camacho, J., and R. C. Johnson, 1988, J. Phys. G **12**, L235.
Hagino, K., N. Takigawa, A. B. Balantekin, and J. R. Bennett, 1995, Phys. Rev. C **52**, 286.
Hagino, K., N. Takigawa, J. R. Bennett, and D. M. Brink, 1995, Phys. Rev. C **51**, 3190.
Hagino, K., N. Takigawa, M. Dasgupta, D. J. Hinde, and J. R. Leigh, 1997, Phys. Rev. C **55**, 276.
Hagino, K., N. Takigawa, and S. Kuyucak, 1997, Phys. Rev. Lett. **79**, 2943.
Halbert, M. L., J. R. Beene, D. C. Hensley, K. Honkanen, T. M. Semkov, V. Abenante, D. G. Sarantites, and Z. Li, 1989, Phys. Rev. C **40**, 2558.
Hänggi, P., P. Talkner, and M. Borkovec, 1990, Rev. Mod. Phys. **62**, 251, and references therein.
Hill, D. L., and J. A. Wheeler, 1953, Phys. Rev. **89**, 1102.
Hinde, D. J., C. R. Morton, M. Dasgupta, J. R. Leigh, R. C. Lemmon, J. P. Lestone, J. C. Mein, and H. Timmers, 1994, *Proceedings of the 7th International Conference on Nuclear Reaction Mechanisms, Varenna, Italy, June 1994*, unpublished.
Hofmann, S., V. Ninov, F. P. Hessberger, P. Armbruster, H. Folger, G. Münzenberg, H. J. Schött, A. G. Popeko, A. V. Yeremin, S. Saro, R. Janik, and M. Leino, 1996, Z. Phys. A **354**, 229.
Hussein, M. S., 1991, Nucl. Phys. A **531**, 192.
Hussein, M. S., M. P. Pato, and A. F. R. de Toledo Piza, 1995, Phys. Rev. C **51**, 846.
Iachello, F., and A. Arima, 1987, *The Interacting Boson Model* (Cambridge University, Cambridge, England).
Imanishi, B., and W. von Oertzen, 1995, Phys. Rev. C **52**, 3249.
Inui, M., and S. E. Koonin, 1984, Phys. Rev. C **30**, 175.
Ishihara, M., N. Takigawa, and S. Yamaji, Eds., 1993, *Heavy-Ion Reactions with Neutron-Rich Beams* (World Scientific, Singapore).
Iwamoto, A., and K. Harada, 1987, Z. Phys. A **326**, 201.
Iwamoto, A., and N. Takigawa, 1989, Phys. Lett. B **219**, 176.
Izumoto, T., T. Udagawa, and B. T. Kim, 1995, Phys. Rev. C **51**, 761.
Jacobs, P. M., and U. Smilansky, 1983, Phys. Lett. B **127**, 313.
Jahnke, U., H. H. Rossner, D. Hilscher, and E. Holub, 1982, Phys. Rev. Lett. **48**, 17.
Jiang, C. L., K. E. Rehm, J. Gehring, B. Glagola, W. Kutschera, M. Rhein, and A. H. Wuosmaa, 1994, Phys. Lett. B **337**, 59.
Kim, K.-H., T. Otsuka, and M. Tohyama, 1994, Phys. Rev. C **50**, R566.
Kodama, T., R. A. M. S. Nazareth, P. Moller, and J. R. Nix, 1978, Phys. Rev. C **17**, 111.
Krappe, H. J., K. Möhring, M. C. Nemes, and H. Rossner, 1983, Z. Phys. A **314**, 23.
Krappe, H. J., J. R. Nix, and A. J. Sierk, 1979, Phys. Rev. C **20**, 992.
Krappe, H. J., and H. Rossner, 1995, in *Low Energy Nuclear Dynamics*, edited by Y. Oganessian *et al.* (World Scientific, Singapore), p. 329.
Kruppa, A. T., P. Romain, M. A. Nagarajan, and N. Rowley, 1993, Nucl. Phys. A **560**, 845.
Kuyucak, S., and I. Morrison, 1988, Ann. Phys. (N.Y.) **181**, 79.
Kuyucak, S., and I. Morrison, 1989a, Ann. Phys. (N.Y.) **195**, 126.
Kuyucak, S., and I. Morrison, 1989b, Phys. Rev. C **41**, 2936.
Kuyucak, S., and I. Morrison, 1993, Phys. Rev. C **48**, 774.
Landowne, S., and J. R. Nix, 1981, Nucl. Phys. A **368**, 352.
Leigh, J. R., M. Dasgupta, D. J. Hinde, J. C. Mein, C. R. Morton, R. C. Lemmon, J. P. Lestone, J. O. Newton, H. Timmers, J. X. Wei, and N. Rowley, 1995, Phys. Rev. C **52**, 3151.
Leigh, J. R., N. Rowley, R. C. Lemmon, D. J. Hinde, J. O. Newton, J. X. Wei, J. C. Mein, C. R. Morton, S. Kuyucak, and A. T. Kruppe, 1993, Phys. Rev. C **47**, R437.
Lemmon, R. C., J. R. Leigh, J. X. Wei, C. R. Morton, D. J. Hinde, J. O. Newton, J. C. Mein, M. Dasgupta, and N. Rowley, 1993, Phys. Lett. B **316**, 32.
Lindsay, R., and N. Rowley, 1984, J. Phys. G **10**, 805.
Möller, P., and A. Iwamoto, 1994, Nucl. Phys. A **575**, 381.
Morton, C. R., Ph.D. Dissertation, Australian National University.
Morton, C. R., M. Dasgupta, D. J. Hinde, J. R. Leigh, R. C. Lemmon, J. P. Lestone, J. C. Mein, J. O. Newton, H. Timmers, N. Rowley, and A. T. Kruppa, 1994, Phys. Rev. Lett. **72**, 4074.
Müller, B., and N. Takigawa, 1987, Ann. Phys. (N.Y.) **173**, 163.
Nagarajan, M. A., A. B. Balantekin, and N. Takigawa, 1986, Phys. Rev. C **34**, 894.
Nagarajan, M. A., C. Mahaux, and G. R. Satchler, 1985, Phys. Rev. Lett. **54**, 1136.
Nomura, T., *et al.*, 1995, *Proceedings of the Tours Symposium on Nuclear Physics II, 1994, Tours, France* (World Scientific, Singapore), pp. 418–427.
Poffe, N., N. Rowley, and R. Lidsay, 1983, Nucl. Phys. A **410**, 498.
Prasad, N. V. S. V., A. M. Vinodkumar, A. K. Sinha, K. M. Varier, D. L. Sastry, N. Madhavan, P. Sugathan, D. O. Kataria, and J. J. Das, 1996, Nucl. Phys. A **603**, 176.
Rehm, K. E., H. Esbensen, J. Gehring, B. Glagola, D. Henderson, W. Kutschera, M. Paul, F. Soramel, and A. H. Wuosmaa, 1993, Phys. Lett. B **317**, 31.
Reisdorf, W., 1994, J. Phys. G **20**, 1297.
Reisdorf, W., F. P. Hessberger, K. D. Hildenbrand, S. Hofmann, G. Münzenberg, K.-H. Schmidt, J. H. R. Schneider, W. F. W. Schneider, K. Sümmerer, and G. Wirth, 1985, Nucl. Phys. A **438**, 212.
Rhodes-Brown, M. J., and V. E. Oberacker, 1983, Phys. Rev. Lett. **50**, 1435.
Rowley, N., 1992, Nucl. Phys. A **538**, 205c.

Rowley, N., A. Kabir, and R. Lindsay, 1989, J. Phys. G **15**, L269.
Rowley, N., J. R. Leigh, J. X. Wei, and R. Lindsay, 1993, Phys. Lett. B **314**, 179.
Rowley, N., G. R. Satchler, and P. H. Stelson, 1991, Phys. Lett. B **254**, 25.
Rowley, N., H. Timmers, J. R. Leigh, M. Dasgupta, D. J. Hinde, J. C. Mein, C. R. Morton, and J. O. Newton, 1996, Phys. Lett. B **373**, 23.
Sahm, C.-C., H.-G. Clerc, K.-H. Scmidt, W. Reisdorf, P. Armbruster, F. P. Hessberger, J. G. Keller, G. Münzenberg, and D. Vermeulen, 1985, Nucl. Phys. A **441**, 316.
Sagawa, H., Nguyen van Giai, N. Takigawa, M. Ishihara, and K. Yazaki, 1995, Z. Phys. A **351**, 385.
Satchler, G. R., 1991, Phys. Rep. **199**, 147.
Schicker, R., N. Alamanos, P. Braun-Munzinger, J. Stachel, and L. Waters, 1988, Phys. Lett. B **206**, 9.
Scholten, O., 1991, in *Computational Nuclear Physics*, edited by K. Langanke, J. A. Maruhn, and S. E. Koonin (Springer-Verlag, New York).
Stefanini, A. M., 1994, in *Proceedings of the International Workshop on "Heavy-Ion Fusion: Exploring the Variety of Nuclear Properties," Padua, Italy, May 25–27, 1994* (World Scientific, Singapore).
Stefanini, A. M., D. Ackermann, L. Corradi, J. H. He, S. Beghini, G. Montagnoli, F. Scarlassara, and G. F. Segato, 1995a, Acta Phys. Pol. B **26**, 503.
Stefanini, A. M., D. Ackermann, L. Corradi, J. H. He, G. Montagnoli, S. Beghini, F. Scarlassara, and G. F. Segato, 1995b, Phys. Rev. C **52**, 1727.
Stefanini, A. M., D. Ackermann, L. Corradi, D. R. Napoli, C. Petrache, P. Spolaore, P. Bednarczyk, H. Q. Zhang, S. Beghini, G. Montagnoli, L. Mueller, F. Scarlassara, G. F. Segato, F. Soramel, and N. Rowley, 1995c, Phys. Rev. Lett. **74**, 864.
Stefanini, A. M., L. Corradi, D. Ackermann, A. Facco, F. Gramegna, H. Moreno, L. Mueller, D. R. Napoli, G. F. Prete, P. Spolaore, S. Beghini, D. Fabris, G. Montagnoli, G. Nebbia, J. A. Ruiz, G. F. Segato, C. Signorini, and G. Viesti, 1992, Nucl. Phys. A **548**, 453.
Stefanini, A. M., J. Wu, L. Corradi, G. Montagnoli, H. Moreno, Y. Nagashima, L. Mueller, M. Narayanasamy, D. R. Napoli, P. Spolaore, S. Beghini, F. Scarlassara, G. F. Segato, F. Soramel, C. Signorini, H. Esbensen, S. Landowne, and G. Pollarolo, 1990, Phys. Lett. B **240**, 306.
Stokstad, R. G., Y. Eisen, S. Kaplanis, D. Pelte, U. Smilansky, and I. Tserruya, 1980, Phys. Rev. C **21**, 2427.
Stokstad, R. G., D. E. DiGregorio, K. T. Lesko, B. A. Harmon, E. B. Norman, J. Pouliot, and Y. D. Chan, 1989, Phys. Rev. Lett. **62**, 399.
Stokstad, R. G., and E. E. Gross, 1981, Phys. Rev. C **23**, 281.
Takigawa, N., Y. Alhassid, and A. B. Balantekin, 1992, Phys. Rev. C **45**, 1850.
Takigawa, N., K. Hagino, and M. Abe, 1995, Phys. Rev. C **51**, 187.
Takigawa, N., K. Hagino, M. Abe, and A. B. Balantekin, 1994, Phys. Rev. C **49**, 2630.
Takigawa, N., and K. Ikeda, 1986, in *Proceedings of the Symposium on Many Facets of Heavy Ion Fusion Reactions*, edited by W. Henning *et al.* (Argonne Report ANL-PHY-86-1), pp. 613–620.
Takigawa, N., M. Kuratani, and H. Sagawa, 1993, Phys. Rev. C **47**, R2470.
Takigawa, N., and H. Sagawa, 1991, Phys. Lett. B **265**, 23.
Takigawa, N., H. Sagawa, and T. Shinozuka, 1992, Nucl. Phys. A **538**, 221c.
Takigawa, N., and T. Shinozuka, 1992, in *Proceedings of the 18th INS International Symposium on Physics with High Intensity Hadron Accelerators, Tokyo, March 14–16, 1990*, edited by S. Kubono and T. Nomura (World Scientific, Singapore).
Takigawa, N., S. Yoshida, K. Hagino, and S. K. Patra, 1995, Nucl. Phys. A **588**, 91c.
Tanimura, O., 1987, Phys. Rev. C **35**, 1600.
Tanimura, O., J. Makowka, and U. Mosel, 1985, Phys. Lett. B **183**, 317.
Thompson, I. J., M. A. Nagarajan, J. S. Lilley, and B. R. Fulton, 1985, Phys. Lett. B **157**, 250.
Timmers, H., J. R. Leigh, M. Dasgupta, D. J. Hinde, R. C. Lemmon, J. C. Mein, C. R. Morton, J. O. Newton, and N. Rowley, 1995, Nucl. Phys. A **584**, 190.
Tsukada, M., S. Kobayashi, S. Kurihara, and S. Nomura, Eds., 1993, *Proceedings of the 4th International Symposium on Foundations of Quantum Mechanics*, JJAP Series 9 (Japanese Journal of Applied Physics Publication Office, Tokyo).
Vandenbosch, R., 1992, Annu. Rev. Nucl. Part. Sci. **42**, 447.
Vandenbosch, R., T. Murakami, C.-C. Sahm, D. D. Leach, A. Ray, and M. J. Murphy, 1986a, Phys. Rev. Lett. **56**, 1234.
Vandenbosch, R., T. Murakami, C.-C. Sahm, D. D. Leach, A. Ray, and M. J. Murphy, 1986b, Phys. Rev. Lett. **57**, 1499.
Vaz, L. C., J. M. Alexander, and G. R. Satchler, 1981, Phys. Rep. C **69**, 373.
von Oertzen, W., and W. Nöremberg, 1973, Nucl. Phys. A **207**, 113.
Wei, J. X., J. R. Leigh, D. J. Hinde, J. O. Newton, R. C. Lemmon, S. Elfstrom, J. X. Chen, and N. Rowley, 1991, Phys. Rev. Lett. **67**, 3368.
Wong, C. Y., 1973, Phys. Rev. Lett. **31**, 766.
Wu, J. Q., G. Bertsch, and A. B. Balantekin, 1985, Phys. Rev. C **32**, 1432.
Wuosmaa, A. H., R. R. Betts, B. B. Back, M. P. Carpenter, H. Esbensen, P. B. Fernandez, B. G. Glagola, Th. Happ, R. V. F. Janssens, T. L. Khoo, E. F. Moore, and F. Scarlassara, 1991, Phys. Lett. B **263**, 23.
Yoshida, A., N. Aoi, T. Fukuda, M. Hirai, M. Ishihara, H. Kobinata, Y. Mizoi, L. Mueller, Y. Nagashima, J. Nakano, T. Nomura, Y. H. Pu, F. Scarlassara, C. Signorini, and Y. Watanabe, 1995, Nucl. Phys. A **588**, 109c.